NASA CR-111976

DEVELOPMENT OF ALUMINUM ALLOY COMPOUNDS FOR ELECTROLUMINESCENT LIGHT SOURCES

by

R. J. Chicotka
L. M. Foster
M. R. Lorenz
A. H. Nethercot
G. D. Pettit

May 31, 1971

Prepared under Contract No. NAS 12-2169 by
IBM Thomas J. Watson Research Center
Yorktown Heights, New York 10598

Langley Research Center

NATIONAL AERONAUTICS AND SPACE ADMINISTRATION

TABLE OF CONTENTS

DEVELOPMENT OF ALUMINUM ALLOY COMPOUNDS FOR ELECTROLUMINESCENT LIGHT SOURCES

By R. J. Chicotka, L. M. Foster, M. R. Lorenz, A. H. Nethercot, and G. D. Pettit

INTRODUCTION

The objective of this report is to describe the work done under Contract NAS 12-2169 between May 28, 1969 and May 15, 1971 on the development of aluminum alloy compounds for electroluminescent light sources and other device applications. It will broadly cover the preparation of these wide band gap semiconductors, their physical properties (particularly their band structures), work done on the fabrication of diode structures from these alloys, and the electrical and light emitting properties of these diodes.

A chief motivation of this work was that, in order to improve the visibility of electroluminescent diodes, it is important that the light emitted have a frequency closely matching that at which the human eye has its maximum sensitivity. This can be accomplished in an optimum fashion by using a semiconductor material which has a band gap substantially larger than this frequency and which can be doped with efficient radiative recombination centers to which the injected carriers will be fairly deeply bound such that the emitted light has this optimum frequency. Two such materials are the ternary alloys (Ga,Al)P and (In,Al)P. In addition to this interest in the light emitting properties of these materials, little was previously known about their basic chemical properties, their stability in the atmosphere, their physical properties, the behavior of dopants, and the difficulties involved in fabricating devices and device structures from them.

It was also practicable during the course of this work to study the similar alloys, (Ga,Al)As and (In,Al)As, in more detail than had previously been possible with little additional expenditure of effort.

PHASE DIAGRAMS

A complete understanding of the III-V semiconductor alloys would require a very extensive theoretical and experimental investigation of all of the thermodynamic properties of these systems. Much of the basic information that would be necessary for such a study is not yet available. Nevertheless, a considerable insight into the nature of these systems can be gotten from the interpretation of certain features of the temperature-composition diagrams that have been determined.

The melting points and dissociation pressures of the ternary alloys involving AlP are very high and it has not yet been possible to determine the temperature-composition diagrams in much detail. However, for these materials,

some information on the end members is either available or has been found during the course of the contract work. This data along with similar data on the arsenic alloy end members is presented in Table I.

A new and rapid method of obtaining solidus curves (i.e., the composition of the solid that can be grown from the melt at various temperatures) has recently been developed at our laboratory.[1] Using these techniques, it has been possible to obtain reliable data on the solidus curves of the (Ga,Al)As and the (In,Al)As ternary systems in the course of the contract work. Since these systems should be rather similar to the (Ga,Al)P and the (In,AlP) systems and since extensive work[2] has been done separately from the contract on other homologous systems such as the (In,Ga) V alloys (with V = Sb,As,P), it is possible to draw some general inferences about the expected behavior of the (Ga,Al)P and (In,Al)P systems that should be of importance in understanding the crystal growth of these systems.

In general, it has been found that there is a large difference between the composition of the solid which can be formed at a given temperature and the composition of the liquid from which it is grown. Such solidus and liquidus curves are shown in Fig. I for the alloy system (In,Ga)P.[2] These experimental curves show a substantially larger difference between the solidus and liquidus than would have been predicted if the rules of ideal solution mixing had been obeyed. This causes the experimental solidus curve to be much flatter on the InP rich side and to exhibit a sharp "knee" on the GaP rich side of the diagram. For the general (A,B)C compound, where A and B are group III elements and C is a group V element, these features become more pronounced the smaller the element C is or, more importantly, the greater the disparity in covalent radii between elements A and B. Thus, for both reasons, the departure of (In,Ga)P from ideality is greater than for (Ga,Al)As, as can be seen from the diagram[3] for (Ga,Al)As shown in Fig. II. The solidus curve[4] for (In,Al)As shown in Fig. III also exhibits features characteristic of a substantial departure from ideality which is caused by the difference in the covalent radii of In and Al of about $\sim$ 13%

It would be expected that the solidus and liquidus curves for (Ga,Al)P should be similar to those for (Ga,Al)As, whereas those for (In,Al)P should be rather similar to those for (In,Al)As and (In,Ga)P.

A number of conclusions can be drawn from the shapes of the experimental temperature-composition diagrams of these pseudobinary III-V alloy systems. All those investigated show complete miscibility in the liquid and in the solid. In addition, even for (In,Al)P, examinations of crystals containing the complete range of compositions showed no evidence of second phase formation.

If experimental data for both the liquidus and solidus boundaries are available and certain parameters of the pure end components are known, the departure of the systems from "ideal" behavior can be calculated and certain inferences can be made from the nature and magnitude of this departure. The

TABLE I

Melting Points and Dissociation Pressure of End Member III-V Compounds

	Melting Point	Dissociation Pressure
AlP	> 1850°C[1]	> 15 atm.[1]
GaP	1485°C[1]	35 atm.[2]
InP	1064°C[3]	18 atm.[3]
AlAs	1770°C[1]	1.7 atm.[1]
GaAs	1238°C[4]	0.9 atm.[4]
InAs	943°C[4]	0.33 atm.[4]

REFERENCES

1. R. J. Chicotka, experimentally determined, unpublished.

2. D. Richman, J. Phys. Chem. Solids 24, 1131 (1963).

3. J. M. Woodall, private communication.

4. J. van den Boomgaard and K. Schol, Phillips Research Reports #12, 127-40 (1957).

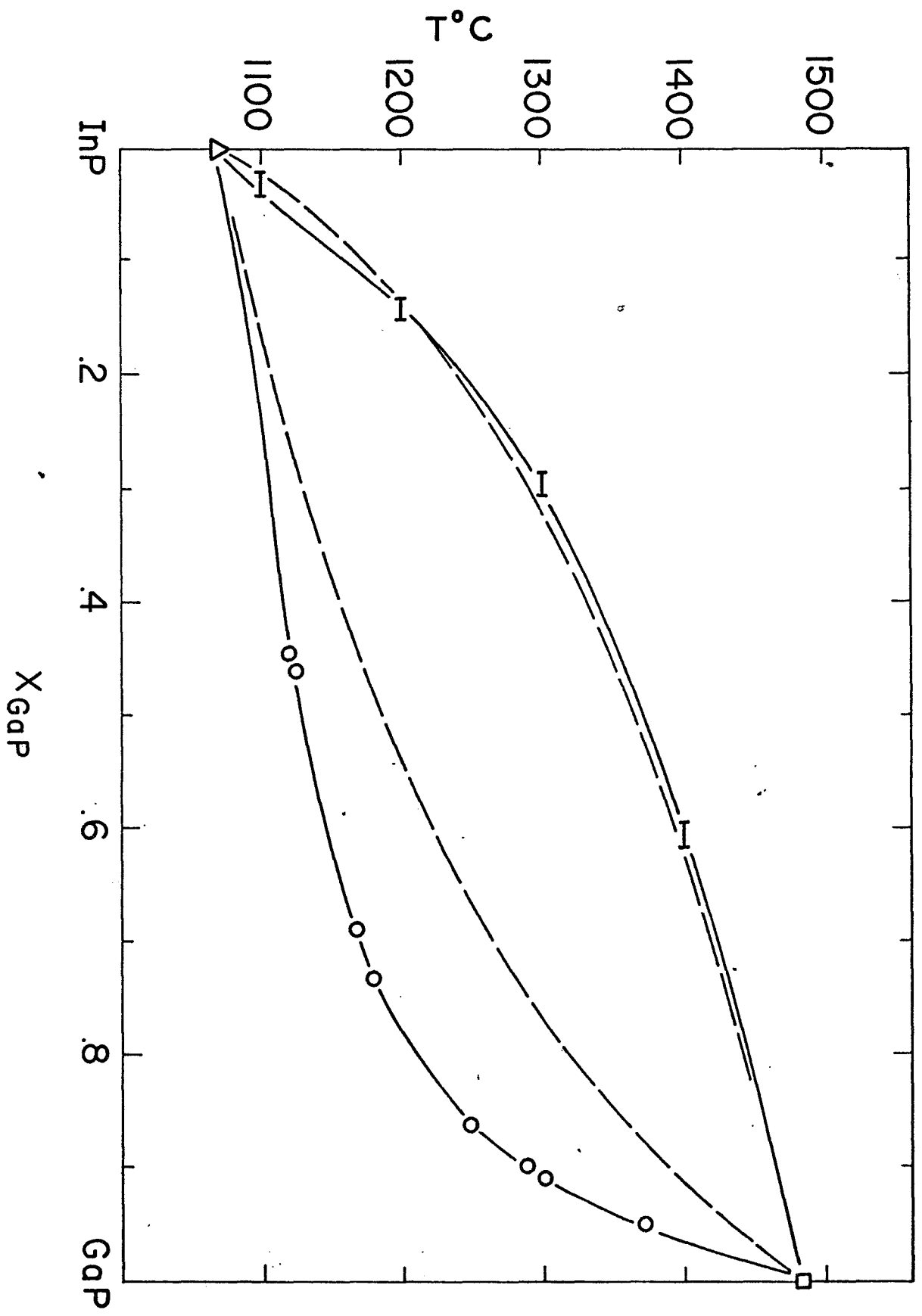

FIGURE I

Solidus and liquidus boundaries of the InP-GaP system.

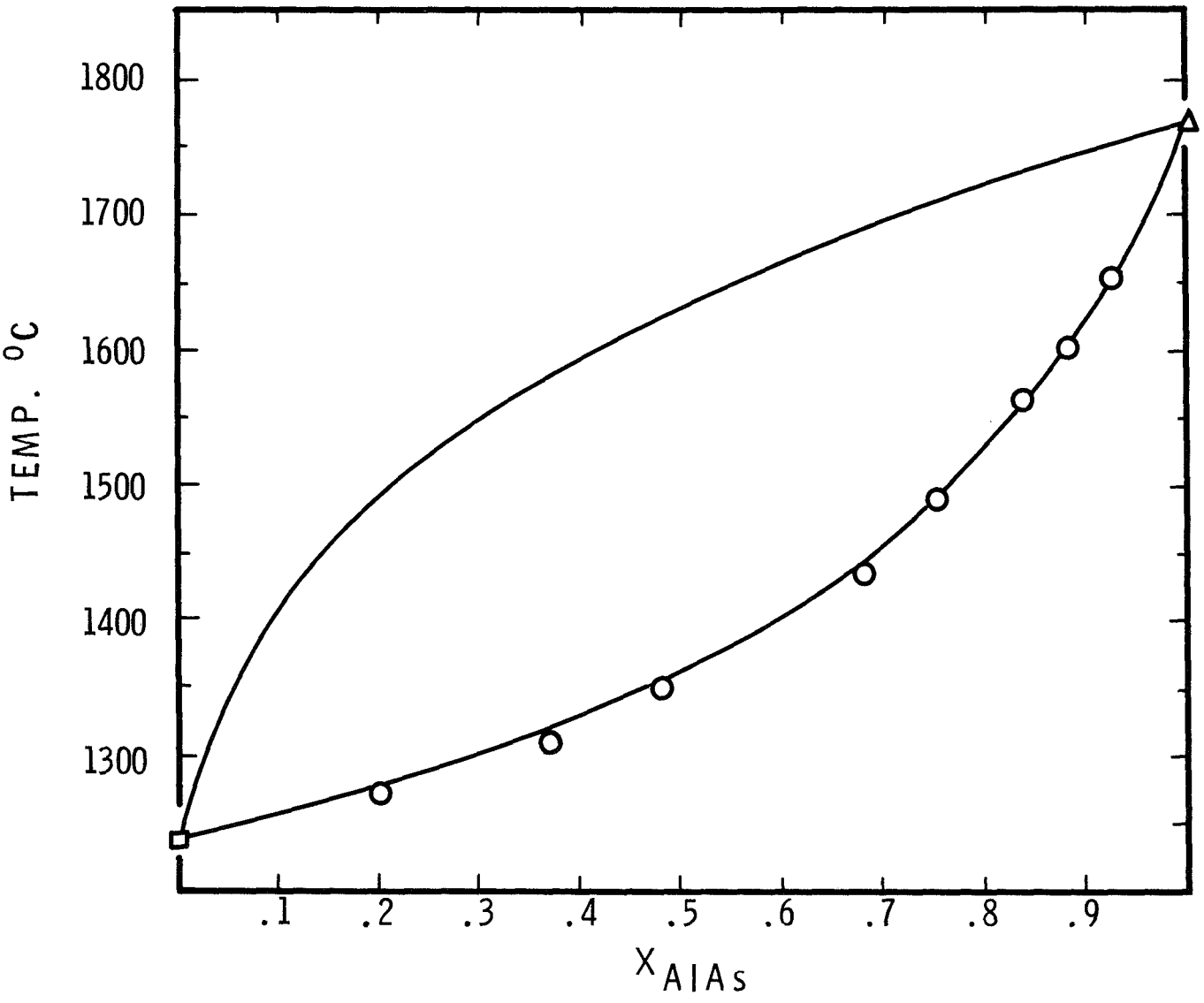

FIGURE II

Solidus and liquidus boundaries of the GaAs-AlAs system. Both solid curves were calculated for ideal solution mixing.

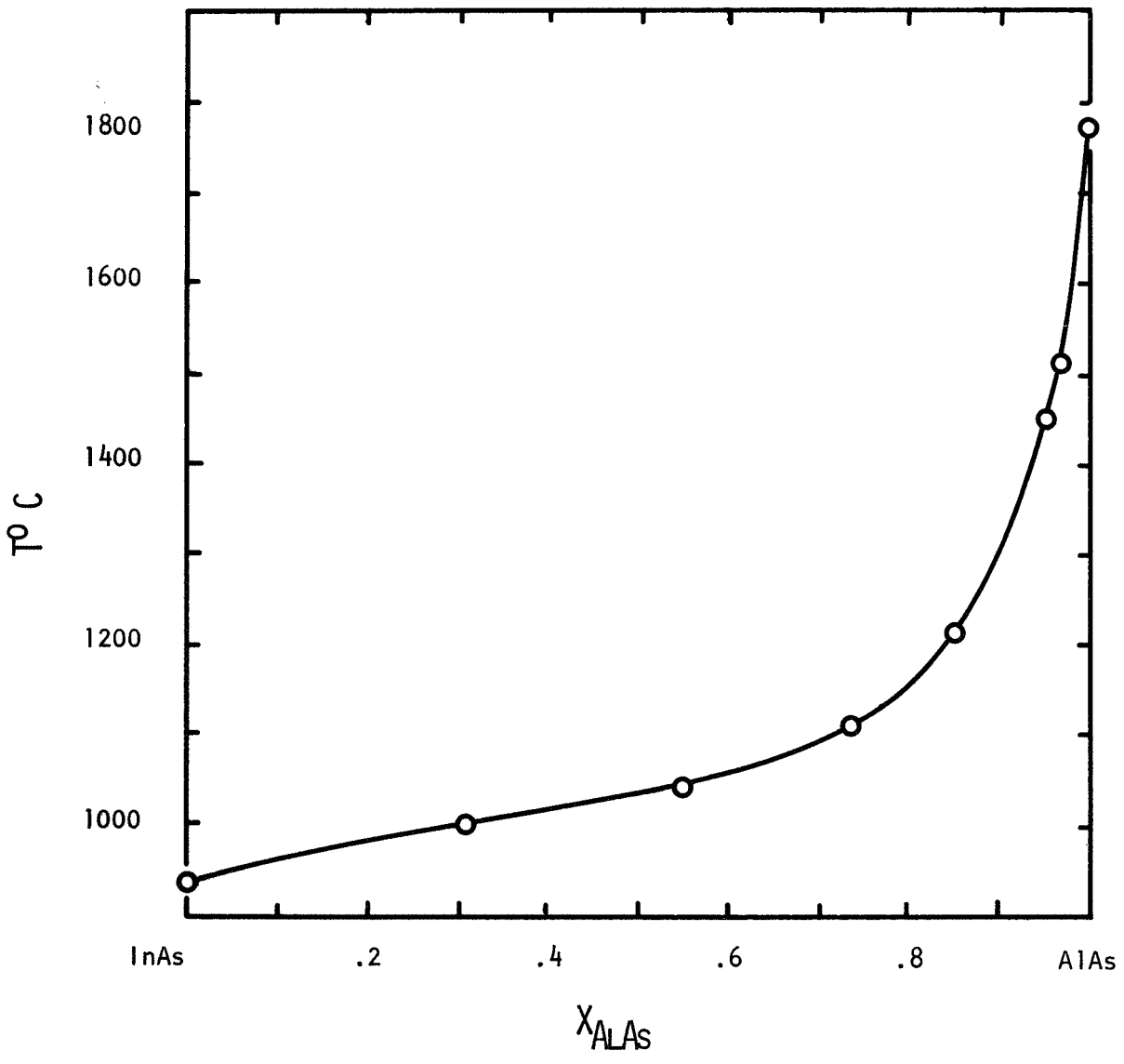

The Solidus Boundary of InAs-AlAs

FIGURE III

theory underlying these calculations is available elsewhere.[2] Although Ref. 2 was concerned with other III-V alloys and the work was not carried out under this contract, it gives the framework within which the somewhat sparse information on the aluminum alloys can be viewed. The pertinent quantity that comes from these theoretical calculations is the parameter B in the term Bx_1x_2, which is defined as the excess free energy of mixing when an alloy is made between the two pure end components of mole fraction x_1 and x_2. This term appears in the expressions for the total free energy of mixing for the liquid and solid:

$$\Delta F^{M(\ell)} = RT(x_1 \ln x_1 + x_2 \ln x_2) + B^{\ell} x_1 x_2$$

and

$$\Delta F^{M(s)} = RT(x_1 \ln x_1 + x_2 \ln x_2) + x_1 L_1 (T/T_1 - 1) + x_2 L_2 (T/T_2 - 1) + B^{s} x_1 x_2,$$

where L_1 and L_2 are the latent heats of fusion of the two pure components and T_1 and T_2 are their melting points.

Both the liquidus and solidus curves are required to derive values for either B^s or B^{ℓ}. These data are not available for the aluminum alloy binary systems, but conclusions based on the three (In,Ga)V alloy systems are applicable.

It is seen (Fig. IV) that the quantity B/RT is essentially independent of x for both the liquid and the solid phases of all three systems. Also, B/RT is substantial for the solid phase of these materials because the lattice parameter mismatch between the two end components is large.

Since Bx_1x_2 is the excess free energy of forming the alloy and B/RT is essentially a constant characteristic of each system, the excess free energy consists almost completely of an excess entropy, $T\Delta S$. Although there is still some uncertainty in the interpretation of these results since the theory of the constitution of molten salts at high temperature is not on a firm foundation, there is a strong implication that there may be a tendency towards formation of some kind of structure in these alloys such as ordering or segregation that increases in extent with the increase in size disparity between the two components of the alloy. Of these large band gap III-V alloy systems, any such tendency should be the largest in the (In,Al)P system and should be rather small for (Ga,Al)P. Although no explicit effects have been observed that can be attributed to such changes in structure, it is possible that more detailed investigations might reveal some difficulties of this general nature. Thus, all other things being equal, these thermodynamic considerations point to alloys such as (Ga,Al)P and, of course, (Ga,Al)As, which have essentially no lattice mismatch, as preferred candidates for semiconductor device investigations. In addition, it is clear that, for those alloys where the lattice constants of both components are similar, substrates of either end member can be used for the deposition of overgrowth layers. For the case of (Ga,Al)P, GaP substrates can conveniently be used, although it

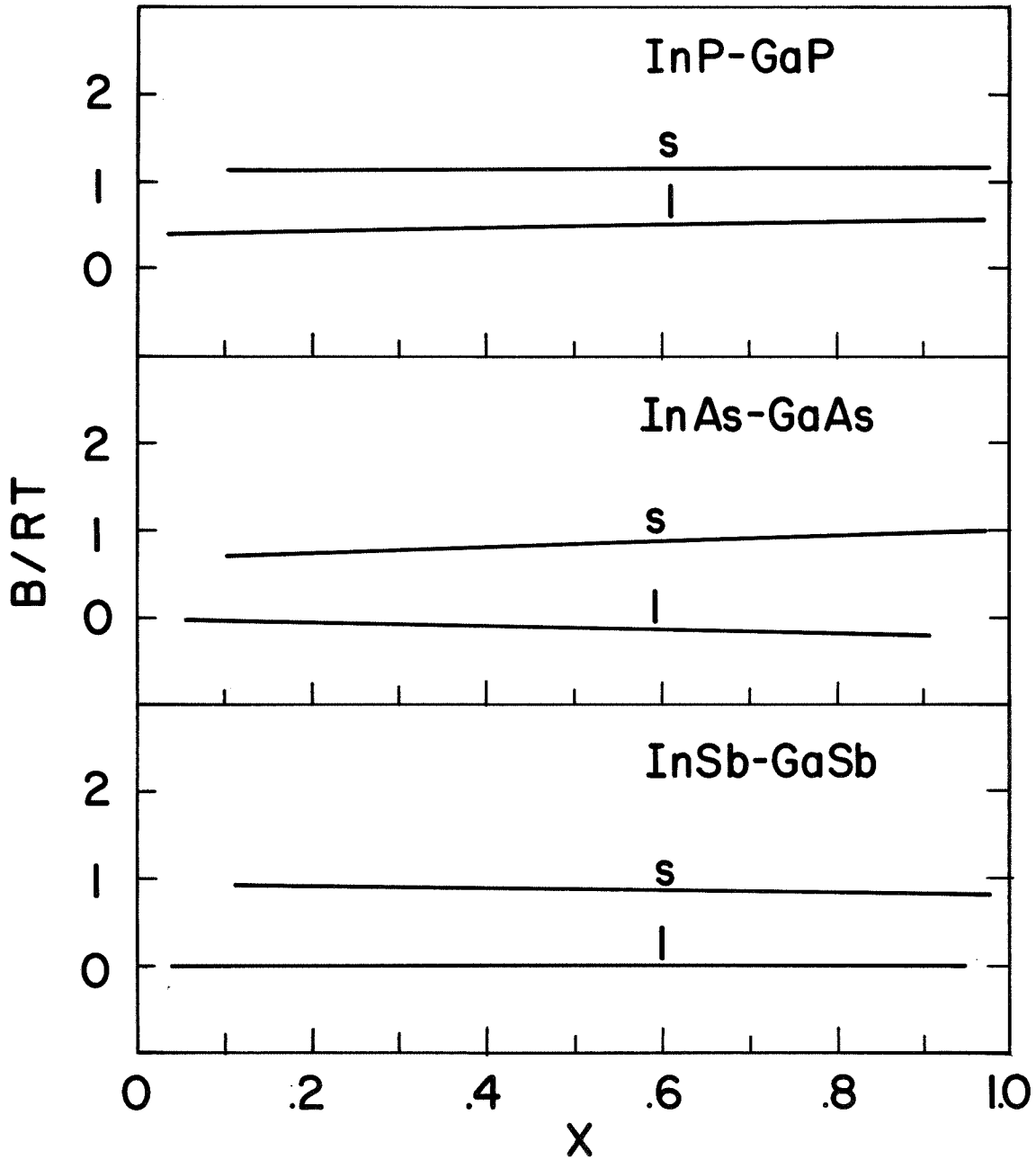

FIGURE IV

B/RT vs composition for III-V alloy systems

is important to note that the initial growth cannot take place under equilibrium thermodynamic conditions.

This analysis gives us some insight into the expected growth behavior of the two ternary systems (Ga,Al)P and (In,Al)P. As mentioned before, the pseudo-binary phase diagram of the (Ga,Al)P system should closely approximate the pseudo-binary (Ga,Al)As system and thus should also approximate that predicted for an ideal solution. On this basis, the composition of (Ga,Al)P material grown from a liquid melt of some given average composition would be expected to change rather slowly and gradually with distance in the direction of solidification. Thus the composition of any small volume selected from a reasonably sized ingot should be very nearly constant. Widely different compositions can be obtained from a single ingot at different positions along its axis.

However, for the (In,Al)P system it would be expected that the solidus and liquidus lines will deviate markedly from ideality similarly to the (In,Al)As system or the (Ga,In)P system. Due to the presence of the very sharp "knee" in the solidus curve, the first-to-freeze solid will be very rich in AlP and deficient in InP. This condition will persist over the major part of the temperature drop and hence most of the ingot will be AlP rich, with a composition varying from perhaps $In_{0.1}Al_{0.9}P$ to $In_{0.2}Al_{0.8}P$. At the last-to-freeze end, the proportion of AlP will decrease very rapidly with distance, giving rise to very inhomogeneous material which would be very difficult to characterize or to use. As will be seen later, alloy compositions in which the AlP mole fraction exceeds 0.44 have an indirect band gap, which is not as favorable from a light emission point of view. Thus, it can be seen that the possible advantages of the direct band gap of (In,Al)P over the indirect band gap of (Ga,Al)P would be very difficult to realize if the material is grown by any bulk method or by liquid phase epitaxy. The only possible way of producing reasonably homogeneous direct band gap (In,Al)P is by chemical vapor deposition and the many substantial technical problems inherent in this approach would be difficult to solve.

On the basis of the phase diagrams, it should be possible to grow highly AlP rich alloys of either (Ga,Al)P or (In,Al)P in homogeneous form. In fact, deviation from ideality is helpful in this respect because the composition of the solid is less dependent on the exact growth temperature and on the exact melt composition than otherwise would have been the case.

In summary, knowledge of the phase diagrams of these aluminum alloy compounds indicates that useful direct band gap (In,Al)P material will be extremely difficult to obtain. In the indirect band gap range, it should be much easier to grow high quality (Ga,Al)P than (In,Al)P due to the availability of suitable substrates and the absence of possible high internal lattice strains.

BULK GROWTH OF POLYCRYSTALLINE ALLOYS AND COMPOUNDS

The synthesis and crystal growth of bulk ingots of the aluminum binary compounds and ternary alloys is desirable for several reasons: First, sufficient material is obtained to obviate the need to evaluate very small platelets or epitaxial layers and to eliminate the problems inherent to their handling. Second, the characteristic parameters such as band gap, composition and transport properties are more easily determinable experimentally and with a greater

degree of confidence in their interpretation. Last, the mixed crystal systems under investigation can be represented by a binary cut in the ternary phase diagram yielding a pseudo-binary diagram and the realized ingots will have a compositional profile which follows approximately the solidus line of the pseudo-binary system under investigation; that is, a single bulk grown ingot will vary in composition along its growth axis thereby enabling many determinations of experimentally important parameters to be performed at various compositions.

The crystal growth technique that we have employed is a modified two-zone Bridgman drop. This method was successfully applied to the growth of the gallium indium phosphide system previously and allowed us to experimentally characterize this mixed crystal system with regard to the energy gap, lattice parameter, etc. and their variation with composition.

Crystals of aluminum arsenide, aluminum phosphide, gallium aluminum phosphide, indium aluminum phosphide and indium aluminum arsenide were prepared by this technique. In addition, crystals of indium phosphide and indium arsenide necessary for subsequent phase diagram studies were also grown in this manner.

A schematic diagram of the apparatus used is shown in Fig. V. It consisted of a heavy wall quartz ampoule (18 mm I.D. x 24 mm O.D.) within which the crucible containing the group III or mixed group III elements and a separate reservoir containing an excess of group V charge were sealed in vacuo. The ampoule was positioned within a vertical tubular furnace as shown. Two separately heated zones were used to independently control the temperatures of the melt and of the group V element reservoir and hence the pressure of the group V element in the reaction tube.

Synthesis and crystal growth were done in situ. Synthesis was achieved by inductively heating the melt contained in the crucible while slowly elevating the temperature of the group V element (and hence its pressure) until the volume of the melt no longer increased with time. For example, for the binary compound aluminum phosphide, the pressure in the system could be held at 15 atmospheres of phosphorus and the melt temperature at 1800°C. For these conditions, we estimate that the composition of the liquid was approximately 0.45 atom fraction of phosphorus. Solidification was obtained either by simultaneously lowering the ampoule and the phosphorus control thermocouple or by raising the RF coil. Clear transparent, single phase crystals were obtained at freezing rates at about 1 cm/hr for the binary compounds and 0.5 cm/hr for the ternary alloys. These ingots were sound and inclusions of the group III metals were not apparent. By a weight gain determination, the average composition of these crystals was equivalent to the value predicted by stoichiometry considerations.

Occasionally, the ingots had a small region at the first-to-freeze portion that was dark in color and rich in the group III element. This was sometimes observed at the tail portion as well. In both cases, this was caused by rapid freezing at the front end due to consitutional supercooling, and at the tail end of the crystal because of rapid loss of RF coupling to the melt. However, in most cases when this occurred, no more than about 10% of the crystal was so affected and at least 35 grams of sound material was obtained in each run.

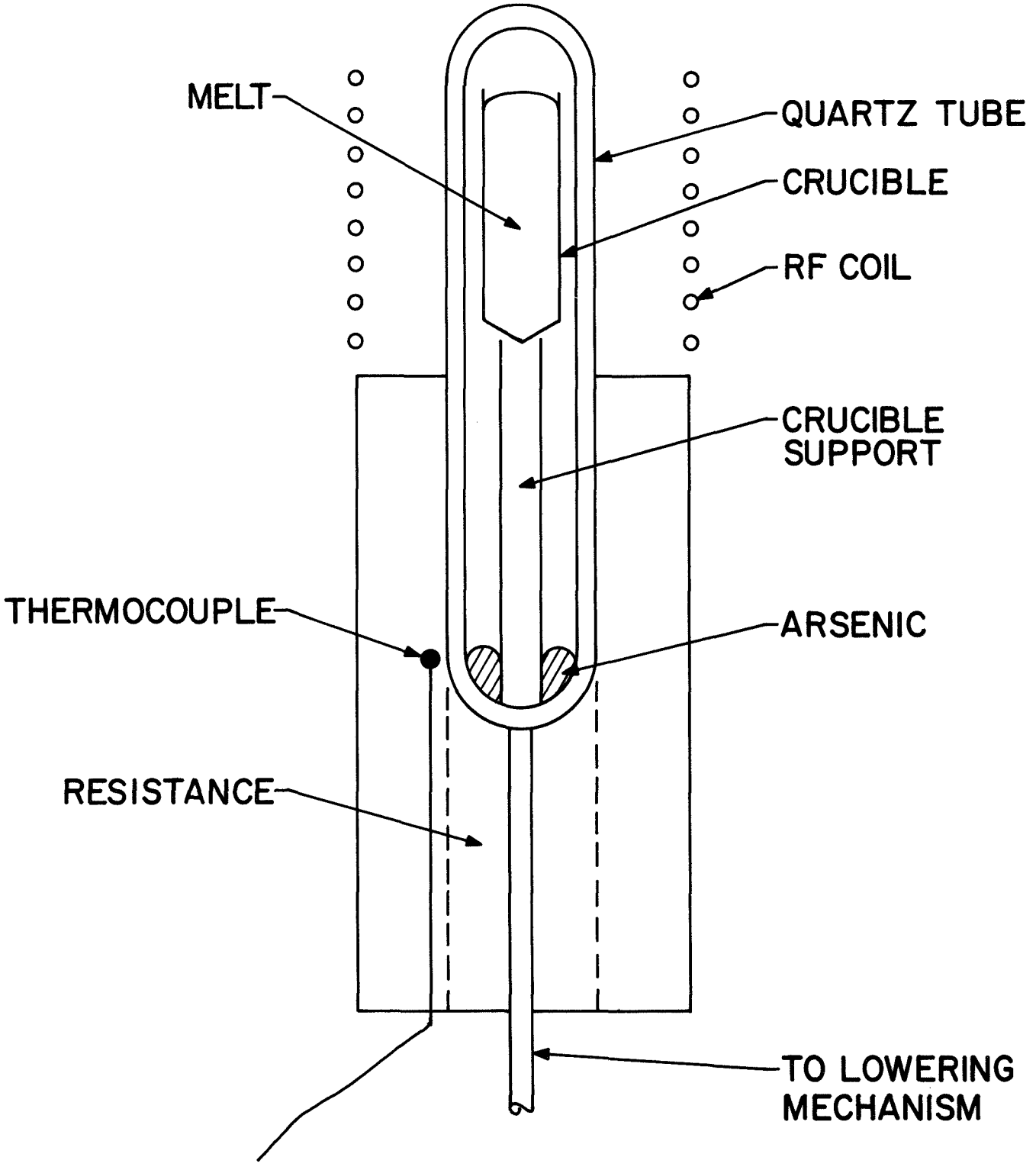

FIGURE V

Modified Bridgman two-zone drop apparatus

The crystals obtained were of circular cross section and had a diameter of 1.5 cm and a length of approximately 7.5 cm. The weights of these ingots corresponded to the stoichiometric weight as defined by the volume times the average density. The compositions of the binary compounds were invariant with respect to the dimensions while the compositions of the ternary compound varied along the growth axis.

The binary compound ingots of aluminum arsenide, aluminum phosphide, indium phosphide and indium arsenide produced by this method were polycrystalline. Figure VI shows a typical cross section of an ingot of AlAs. In general, the crystallites were columnar and were arrayed with the long axis parallel to the direction of growth. Typical grain sizes of individual grains were on the order of 3 x 1 x 1 mm. For the ternary alloys of gallium aluminum phosphide, indium aluminum phosphide and indium aluminum arsenide the grain sizes were typically smaller, being on the order of 1 mm in all dimensions.

Two changes were required to obtain such grain sizes. First, for the binary compounds such as aluminum phosphide, an increase in the reaction temperature and the overpressure of the volatile component tends to bring the system nearer to the stoichiometric liquid. From knowledge of the crystallization process based on past experience on the growth of binary compounds, it should be necessary for optimum single crystal growth to grow from a near stoichiometric liquid or to have the melt slightly enriched with the volatile component.

The second change involved the use of internal radiation shields to reduce the radial heat losses, thus maximizing the temperature gradient along the bulk grown material. Normally without the use of radiation shields the freezing interface during solidification is concave toward the solid phase. Such an interface permits growth of crystallites nucleated at the crucible-melt-solid interface. The use of internal radiation shields tends to reduce such stray nucleation on the sides of the crucible and also should enhance the growth of those grains which have certain favorable growth orientations, thereby increasing their cross sectional areas.

Aluminum phosphide was synthesized and grown using a combination of both methods. The larger grain sizes were obtained when the reaction temperatures and pressures were 1800°C and 15 atmospheres phosphorus than when the growth conditions were 1500°C and 8 atmospheres phosphorus. The resulting ingot was roughly stoichiometric by a weight gain measurement. The grain size was also approximately 3 x 1 x 1 mm. However, a complication arose when further increases in growth temperature were attempted in that a second phase appeared which was identified as boron phosphide. Thus attempts to further increase the grain size by increasing the melt temperature were hampered to some extent by a partial dissolution of the boron nitride crucible and this obviously reduces the chemical purity of the compound.

Estimates of the dependence of melting temperature and dissociation pressure on the melt stoichiometry were made during the synthesis of the AlAs ingots. The aluminum arsenide melt surface was observed with an optical pyrometer during synthesis. Since there is a large difference in the spectral emissivity between solid and liquid aluminum arsenide, it was relatively easy to discern

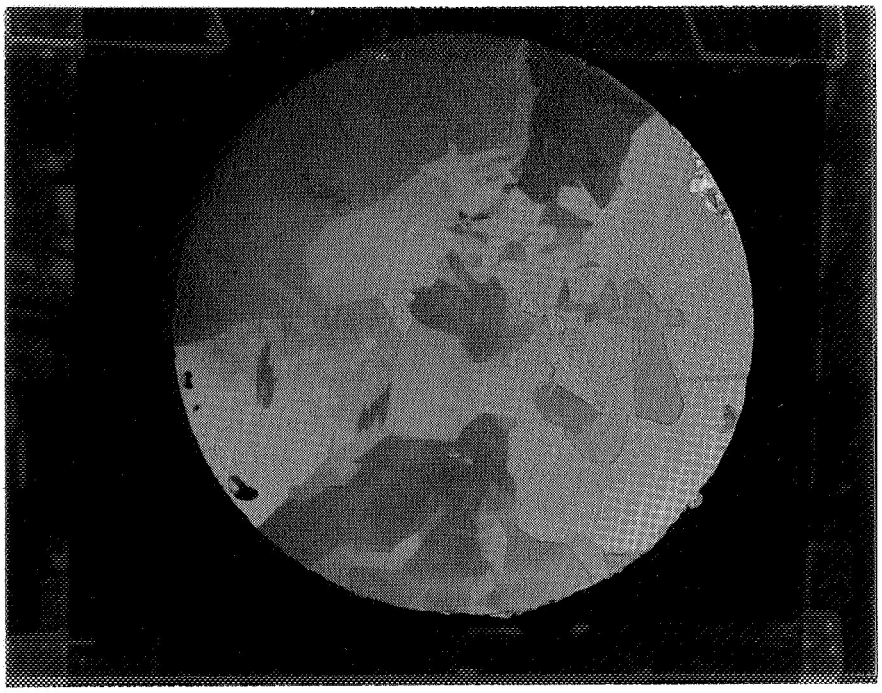

FIGURE VI

Cross section of an AlAs crystal. The diameter of the wafer is 1.5 cm.

and measure the temperature of the solid phase that formed as a function of arsenic pressure. This dependence was obtained by allowing an aluminum melt at some temperature to saturate with arsenic from the vapor phase. Since the specific volume of the solid is greater than the specific volume of the liquid, solid aluminum arsenide forms on the surface of the melt if the arsenic pressure is too high. By alternately allowing the surface of the melt to solidify, by increasing the arsenic pressure in small increments, and then melting the surface by increasing the temperature through small intervals, the dissociation pressure and maximum melting temperature can be found experimentally. The maximum melting temperature corresponds to the condition when the last solid to form is dissolved and no further solidification occurs as a result of changing the arsenic pressure. The dissociation pressure corresponds to that pressure just below the maximum melting point where a solid phase re-forms. The values of these parameters are 1770°C for the maximum melting point and 1.7 atm for the dissociation pressure.

Some observations on representative macro-samples of the binary and ternary crystal systems showed the following:

(1) Gallium aluminum phosphide: The crystal was transparent and varied in color from yellow-green to yellow to yellow-orange to reddish-orange. The composition of the ingots varied both transversely and longitudinally to the growth direction. The variation in composition in any one wafer, however, was gradual from the periphery of the wafer to its center. This was evidenced by a series of concentric rings of varying color. The wafers were easily polished by conventional techniques and showed no degradation after direct exposure to the air or to water.

(2) Indium aluminum phosphide: The crystal was transparent and yellow in color. The composition of the ingot was essentially constant near to that of pure aluminum phosphide and the composition abruptly changed to that of almost pure indium phosphide. Across any one wafer the composition was constant from the periphery to near the center of the ingot. However, a small amount of secondary phase was present in the center of the wafer as evidenced by a sharp discontinuity in the color and the transparency of the crystal. Wafers cut from the crystal which contained more than 20% InP were easily polished by ordinary lapping techniques and showed no rapid degradation on exposure to air or water.

(3) Aluminum phosphide: The entire crystal was transparent and yellow in color. Wafers cut from various sections of the crystal showed no evidence of any second phase material (such as metallic aluminum or an aluminum subphosphide). The grain size of the crystals was appreciably larger than in the mixed crystal systems and was of the order of 2 mm x 2 mm in cross section. These wafers reacted very readily with moisture in the air and immediately upon contact with water yielded aluminum oxide and phosphine. This lack of stability in a normal atmosphere may be inherent in pure AlP although it is possible that by increasing the grain size of this compound it might be more stable.

(4) Aluminum arsenide: The entire crystal was transparent and red-orange in color. There was no evidence of any metallic inclusions and the composition corresponded to the stoichiometric proportions. Again the grain size showed an improvement over the other crystal systems, the smallest grains being of the order of 2 mm x 2 mm in cross section. These wafers reacted slowly when exposed to moisture and more rapidly when in contact with water. Observations on the attack by water were evidenced by a darkening of the grain boundaries and subsequent fracturing of the wafer with the release of arsine. The stability might be improved by enlarging the grain size in the growth process.

(5) Indium phosphide: The ingot was sound and inclusion-free and corresponded to stoichiometric proportions. Wafers cut from the ingot showed a grain size of approximately 1 mm x 1 mm in cross section and suffered no degradation when exposed to moisture or water.

Special handling techniques had to be devised and implemented in the case of the aluminum phosphide and aluminum arsenide. From previous experience in dealing with aluminum compounds we anticipated that they might be unstable in a normal atmosphere. The ingots that we obtained were immediately coated with several millimeters of glycol-phthalate in order to preserve them. The aluminum phosphide and aluminum arsenide coated in this manner were stable in the atmosphere. Wafers were cut from these ingots under kerosene and were stored in dried kerosene. All subsequent lapping operations were done under kerosene or a kerosene petroleum ether mixture. The samples were mounted by first heating glycol-phthalate on a lapping jig immersed in kerosene, heating to 80°C and then applying the sample. This procedure worked very well and the samples suffered no deleterious effects.

A significant result realized by comparison of the physical properties of the aluminum phosphide, gallium aluminum phosphide and indium aluminum phosphide crystals is that additions of gallium or indium to aluminum phosphide stabilizes the compound. The propensity towards degradation through exposure to the atmosphere and to water is greatly reduced. The implication is that ternary aluminum phosphide compounds with very high band gaps which do not decompose in air may be synthesized and grown by this method. Although the binary compounds aluminum phosphide and aluminum arsenide are unstable and react with the moisture in the air or with water unless special precautions are taken in their handling and storage and the ternary compounds aluminum indium phosphide, aluminum gallium phosphide and aluminum indium arsenide are also unstable at high aluminum concentrations, these ternary alloys become progressively less reactive with moisture and water as the concentration of aluminum is monotonically reduced.

A number of samples of aluminum indium phosphide, aluminum gallium phosphide and aluminum indium arsenide were analyzed by atomic absorption spectroscopy to determine their aluminum concentrations. The samples selected to be analyzed were chosen from various sections of the crystal and appeared to be homogeneous with no metallic or second phase inclusions. Samples chosen from the end of the crystal containing less aluminum are shown in the second column of Table II and were quite stable. These samples showed no signs of degradation after

exposure to the atmosphere for periods in excess of fourteen weeks. The samples shown in column three are less stable, showing the formation of a slight patina when left in the atmosphere for a period of a week or longer. The samples shown in column four were selected from the edge of the obviously unstable region of the ingot. These samples degraded rapidly, showing a white aluminum oxide crust when left in the atmosphere longer than approximately ten minutes. However, these wafers can be handled and processed using special techniques. Values of the energy gaps measured for these crystals are given in column five, showing that these crystal compositions are all in the indirect band gap range. From Table II it can be seen that crystals containing less than approximately 90% aluminum are reasonably stable and that gallium may stabilize the aluminum alloys somewhat better than indium. After a storage period of one year or more, it was observed that the (In,Al)P alloys had deteriorated substantially while the (Ga,Al)P alloys were in many cases relatively unaffected.

In order to apply ohmic alloy contacts to electrical devices, it is necessary to have clean oxide-free surfaces. This is especially true in the case of aluminum arsenide. On exposure to the atmosphere aluminum arsenide rapidly develops an impervious oxide film which inhibits efforts to prepare normal alloy contacts.

Two methods of surface preparation have been found which yield clean oxide-free surfaces suitable for electrical contacting: The first method consists of heating a sample of aluminum arsenide coated with cesium fluoride to approximately 600°C under an argon atmosphere. The cesium fluoride melts and completely wets the aluminum arsenide surface, reacting with the surface oxide and thus removing the oxide layer and also part of the aluminum arsenide surface. Surfaces prepared in this manner were easily alloy contacted.

The second method makes use of a well known etchant for III-V compounds: a bromine in methyl alcohol solution. A satisfactory concentration was found to be 2% bromine in methyl alcohol by volume. It was necessary to ultrasonically agitate the etchant so as to remove a scum which appeared on the aluminum arsenide surface. The scum is probably a film of aluminum bromide which adheres to the aluminum arsenide surface.

Samples of aluminum arsenide were analyzed for impurities by mass spectrographic techniques. Samples which were nominally undoped, zinc doped, phosphorus doped and nitrogen doped were included. The following is a summary of the results:

AlAs Sample	Impurities (ppm)						
	B	N	O	Mg	Na	P	Cl
undoped	300	30	10,000	30	30	< 3	10
zinc doped	100	100	3,000	30	30	3	10
phosphorus doped	major ∿ 3%	30,000	10,000	< 3	< 3	major ∿ 1%	10
nitrogen doped	100	30	3,000	10	30	10	10

TABLE II

Sample	Composition of wafer from stable region	Composition of wafer from relatively stable region	Composition of wafer from unstable region	Energy Gap
	$Al_{.78}In_{.22}P$			> 2.3 eV
Aluminum indium phosphide		$Al_{.89}In_{.11}P$		> 2.4 eV
			$Al_{.94}In_{.06}P$	> 2.4 eV
	$Al_{.07}Ga_{0.3}P$			
Aluminum gallium phosphide		$Al_{.92}Ga_{0.8}P$		
			$Al_{.99}Ga_{0.1}P$	
	$Al_{0.5}In_{0.5}As$			
Aluminum indium arsenide		$Al_{.84}In_{.16}As$		> 2.1 eV
			$Al_{.92}In_{.08}As$	> 2.15 eV

These were the only major impurities detected and apparently there seem to be no major differences in the samples that were nominally undoped, zinc doped, and nitrogen doped. The only anomalous result was in the sample doped with phosphorus in which boron becomes a major contaminant. This may be due to the higher growth temperature used in the growth of this aluminum arsenide phosphide pseudo-binary.

A zinc doped and an undoped AlAs sample were also analyzed for impurities by radioactivation analysis. The zinc doped sample had a concentration of 1.3×10^{16} atoms/cc and the undoped sample had less than 10^{14} atoms/cc. The zinc doped sample had been grown from a melt of initial dopant concentration of 6×10^{18} atoms/cc. The very large change in dopant concentration between the melt and the grown crystal probably cannot be accounted for by normal segregation alone. Apparently, the volatile zinc dopant is expelled from the melt due to its relatively large vapor pressure in the melt and it then condenses in a cooler part of the reaction tube. Since most shallow p and n dopants are quite volatile, it will probably be very difficult to dope such aluminum arsenide or aluminum phosphhide melts with either n-type or p-type dopants.

In summary, it has been found possible to grow bulk ingots of these aluminum compounds and alloys which are suitable for various measurements and characterization procedures. The major problems found were difficulties in doping these bulk crystals and variations in composition for the ternary alloys. This compositional variation was particularly severe for direct band gap (In,Al)P. These difficulties should be less serious in the liquid phase epitaxial growth of thin (Ga,Al)P films on GaP substrates and this approach will be discussed later in this report.

BAND STRUCTURE AND OPTICAL PROPERTIES

Although the optical properties of many III-V compounds had been extensively studied at the start of the contract period, there was a lack of definitive data on such basic properties as the fundamental energy gap of AlAs and AlP. To understand the ternary III-V alloys containing Al it was also necessary to study the binary compounds AlAs and AlP. For a complete understanding, not only the fundamental energy gap is important but also higher lying conduction band minima. Using optical measurements, the absorption edge of AlAs and AlP was measured at 300°K and 2°K. By detailed analysis of the onset region, the fundamental gap was determined. From a theoretical analysis of the absorption beyond the onset region the higher lying direct gap of AlAs was also obtained.

The direct transition region of the $In_{1-x}Al_xP$ and $In_{1-x}Al_xAs$ alloy systems was studied using the electron microprobe coupled with cathodoluminescence measurements. From this investigation the energy gap dependence on composition was determined and the important crossover point, the point where the direct gap and the indirect gap are degenerate, was located.

Optical Absorption and Photoemission of AlAs and AlP.- The optical transmission of AlAs was measured on samples of various thicknesses from 0.58 cm to 0.028 cm. The AlP data were obtained from samples 0.127 to 0.032 cm thick. The absorption coefficients, α , were calculated from the transmission, T , using the expression:

$$T = \frac{(1-R)^2 e^{-\alpha x}}{1-R^2 e^{-2\alpha x}} \qquad (1)$$

where R is the reflectivity. We used 0.28 for R. This value was determined for AlAs by an apparent thickness measurement under microscopic examination which gave an index of refraction of 3.3 for light in the yellow to green spectral region. This value has since been confirmed.[5] All the crystals measured had appreciable transmission losses in wavelength regions far removed from the absorption edge. We assume that scattering from grain boundaries and the imperfect surfaces can account for these losses since they were essentially independent of wavelength. Therefore, these losses were subtracted as background absorption.

In Fig. 7 we have plotted the square root of the absorption coefficient, $\alpha^{1/2}$, as a function of the photon energy $h\nu$ for AlAs at 2° and 300°K, and for AlP at 6°K and 300°K. The data for AlAs at 2°, 77°K and 145°K are also shown in Fig. 8, but on an expanded energy scale. It can be seen in Fig. 7 that for AlAs at absorption coefficients above 10 cm^{-1} the dependence on photon energy is given by:

$$\alpha = A(h\nu - E_o)^2 \qquad (2)$$

This is the dependence expected for indirect optical transitions and is in agreement with the results and interpretation of Mead and Spitzer.[6] For indirect transitions we also expect to see at low absorption coefficients structure due to free exciton absorption assisted by various phonons.[7] This structure should be more clearly observed at low temperatures, e.g. in Fig. 8. The results on AlP in Fig. 7 appear similar to those on AlAs in the dependence on photon energy, although the structure near 2.5 eV is appreciably less well defined. We conclude from these data that both AlAs and AlP have lowest conduction band minima not at k = (0,0,0) and that the absorption edge is dominated by indirect transitions.

We now consider the structure in the absorption edge region of AlAs at low temperature, shown in Fig. 8, for the determination of the energy gap. We start the analysis with the absorption line marked A in the 2°K data. This is a bound exciton line of unknown origin but believed to be due to an isoelectronic impurity. This line has four relatively weak phonon replicas at approximately 13, 27, 42 and 50 meV higher energy. From the energies of the four observed phonons we cannot decide whether the exciton is bound to a defect associated with conduction band minima in the (1,0,0) or (1,1,1) direction. However we can designate these phonons in the order TA, LA, TO and LO respectively. The line A and its phonon replicas are marked accordingly.

A striking feature of the absorption edge is an absorption threshold about 6 meV above the A line and each of its associated phonon replicas. If we assume that the A line is a zero phonon process, then the five absorption thresholds correspond to E_{gx}, E_{gx} + TA, E_{gx} + LA, E_{gx} + TO and E_{gx} + LO where E_{gx} is the exciton energy gap. The four phonon-assisted components are expected

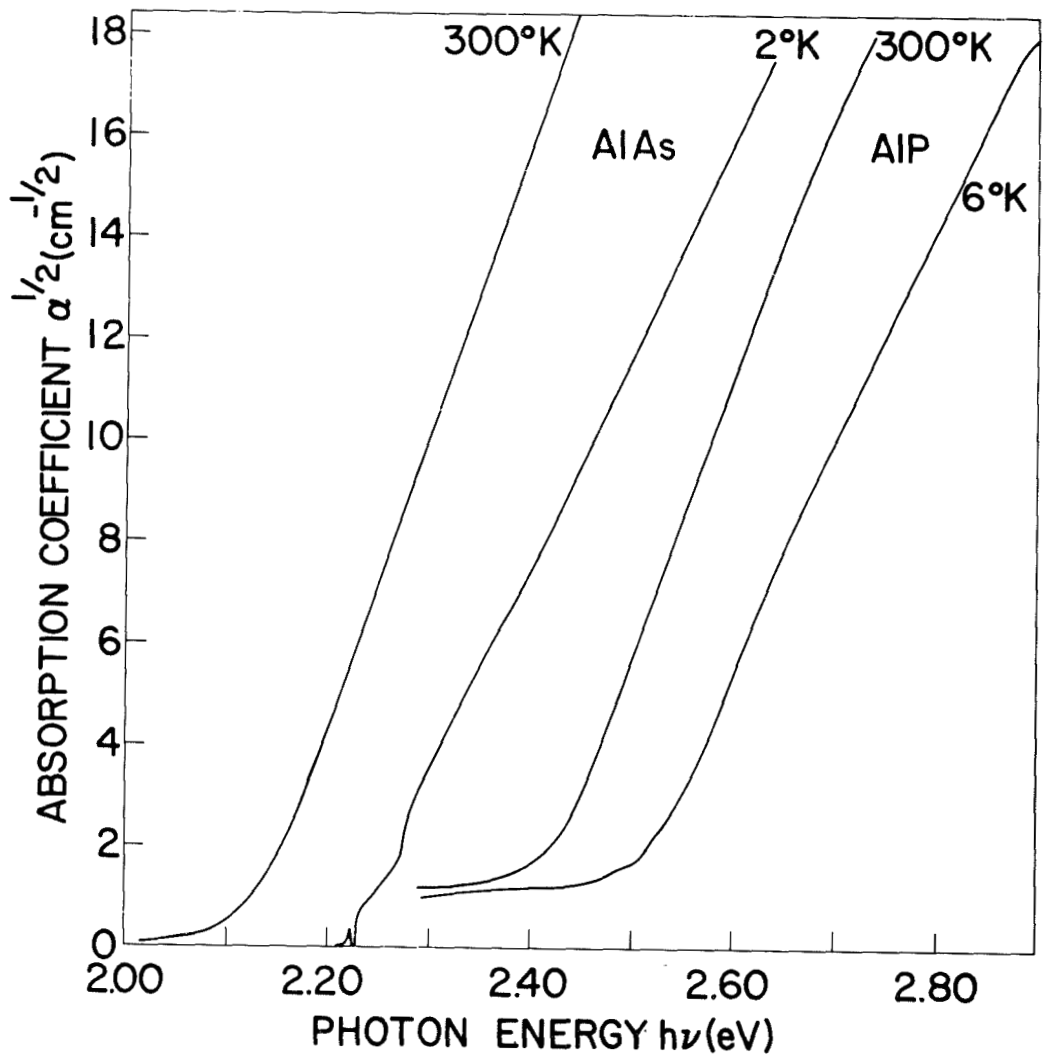

FIGURE VII

The Optical absorption spectrum of AlAs and AlP crystals

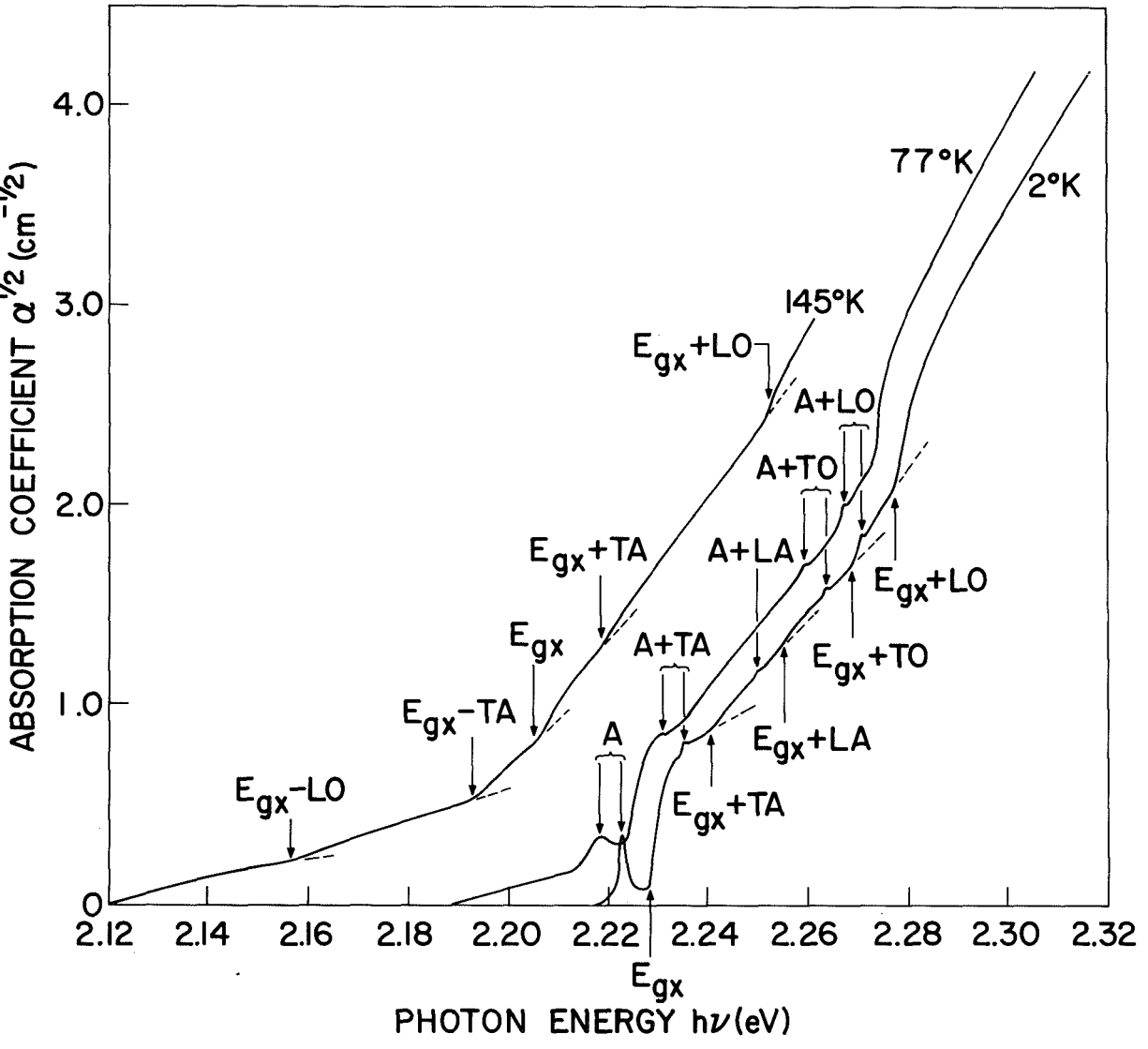

FIGURE VIII

The near-edge absorption spectrum of AlAs at 2°, 77°, and 145°K. The exciton energy gap, E_{gx} and the bound exciton line, A, and their phonon replicas are indicated.

for an indirect transition material according to the theory of Elliott.[7] The somewhat surprising feature is the observation of a zero phonon free exciton absorption. However this phenomenon has been observed previously[8] in GaP when doped with Sb, Bi or As, presumably due to weak interactions of the free excitons with these dopants. On the basis of the experimental results in AlAs the localization energy for the A bound exciton is about 6 meV. It is probable that the defect responsible for the A line absorption is also the center which leads to the no-phonon free exciton component since these features have the same relative strength for crystals from several different ingots, although a priori they need not be the same.

It is interesting to note that the no-phonon free exciton absorption component is relatively strong compared to the TA, LA and TO phonon assisted components. Only the component E_{gx} + LO appears comparable to E_{gx}. However, by comparing the relative strengths of the phonon-assisted bound exciton absorption and the corresponding phonon-assisted free exciton components we conclude that the latter are produced largely by intrinsic transitions. The strength of these intrinsic transitions, however, is less than in GaP. This is consistent with larger energy denominators in the transition matrix elements, a consequence of the larger $\Gamma_1 - X_1$ energy separation in AlAs.

Since the intrinsic exciton absorption is dominated by the LO phonon-assisted component and on the basis of selection rules, we suggest that the conduction band minima occur at X or at least near the zone boundary in the (1,0,0) direction. Recently the suggested conduction band symmetry was confirmed from measurement of the longitudinal piezoresistance of $Ga_{1-x}Al_xAs$ in the high Al content range.[9]

Our model places the 2°K exciton energy gap in AlAs at 2.228 ± 0.001 eV. If our model is correct we should observe at higher temperature the anti-Stokes line of the strong LO component. The absorption coefficient at 145°K is also shown in Fig. 8 and shows both the Stokes and anti-Stokes component of the TA and LO phonons, thus lending further support to our model. If we assume a free exciton binding energy for AlAs of about 0.01 eV consistent with a similar value in GaP[10] and Si,[11] the energy gap for AlAs at 2°K is 2.238 eV. From the measurements at higher temperatures we deduce the energy gaps given in Table II. The 300°K value of 2.16 eV is in reasonable agreement with the experimental values reported previously (∿ 2.1 eV).[6,12] These results on AlAs have been published separately.[13]

The threshold absorption energy at the fundamental edge in AlP is masked by a broad absorption band or tail of unknown origin extending almost 0.5 eV to lower energy. This band appears to be due to absorption in the bulk of AlP since the low energy edge of the broad band (not shown in Fig. 7 for sake of clarity) shifts to lower energy with increasing temperature similar to the shift of the fundamental edge. If we extrapolate the broad band into the absorption edge region and the straight line portion of the absorption edge toward $\alpha^{1/2} = 0$ we find the extrapolated lines cross at ∿ 2.50 eV for the 6°K data and at 2.425 eV for the 300°K data. The qualitative similarity in the fine structure of the low temperature AlAs and AlP spectra in Fig. 7 leads

to the suggestion that the broadened threshold near 2.57 eV (not easily seen in Fig. 7) in the AlP spectrum is due to the onset of LO phonon-assisted indirect transitions. The fundamental lattice vibrational energies of AlP should be of the order of those in Si, as evidenced by the zone center frequencies obtained from Raman scattering.[14] The energy of the LO phonon relevant to indirect transitions is probably $\sim$ 60 meV. Thus the exciton energy gap of AlP is $\sim$ 2.51 eV at 6°K if we have correctly identified the 2.57 eV absorption threshold. Note that there is a threshold near 2.51 eV in the 6°K AlP spectrum in Fig. 7, further emphasizing the similarity with AlAs. From these considerations, we suggest the values of E_g for AlP shown in Table III. There is no evidence for direct optical transitions to the Γ_1 minimum in AlP, suggesting that it lies at least 2.9 eV above the valence band maximum at 6°K.[1]

The indirect interband optical absorption of GaP and AlAs beyond the absorption threshold region has been measured and analyzed at phonon energies up to 2.85 and 3.05 eV respectively. The measurements were made at low temperatures and included absorption constants up to approximately $3 \cdot 10^3$ cm^{-1}.[3] Deviations from a simple indirect absorption law are understandable in terms of the effects of higher conduction minima on the absorption. This deviation in the absorption below the direct band gap can be explained by the decreasing energy denominators involving the Γ_2 states at the center of the Brillouin zone. The analysis of this increase yields direct band gaps of 2.86 eV for GaP and 3.13 eV for AlAs at 6°K.[15] In GaP and AlAs there is evidence of a higher set of extrema giving rise to an additional indirect absorption component 0.34 and 0.20 eV respectively above that due to the lowest conduction minima. The strength of the absorption due to these higher valleys indicates that they contain states of X_3 symmetry.[15]

Further information on these compounds has been obtained from photoemission studies. The best data were obtained for AlAs, where donor-acceptor pair bands have been observed.

Undoped AlAs typically exhibits two such pair bands, one at about 2.15 eV and the other at about 2.10 eV. Samples doped intentionally with Zn show an additional band at about 2.065 eV. The various possible origins of these bands are a single donor and two acceptors, a single acceptor and two donors, or (less likely) two acceptors and two donors (in the latter case one would probably expect four pair bands). We cite as evidence for this conclusion the fact that the intensity ratio between the 2.15 eV band (the peak energy varies depending on sample from 2.145 to 2.155 eV) and the 2.10 eV band (2.095 - 2.105 eV) is not constant from sample to sample. In fact, some samples show the 2.100 eV peak to be the dominant one. Further evidence for these two peaks having separate origins, and thus not being phonon replicas, is the observation of individual pair lines on the higher energy side of both peaks. If one peak had been the phonon replica of the other, the phonon replicas of the individual pair lines should have been too weak to be observed.

The spectrum of a Zn doped sample is shown in Fig. 9 (hole concentration $\sim 3 \times 10^{17}$/cc).[17] A series of sharp pair lines not present in the undoped sample is evident. The expression for such donor-acceptor pair recombination is:

TABLE III

Energy Gaps of AlAs and AlP

Material	T(°K)	E_{gx}(eV)	E_g(eV)
AlAs	2°	2.228 ± 0.001	2.238
	77°	2.223 ± 0.002	2.233
	145°	2.205 ± 0.002	2.215
	300°		2.16
AlP	6°	2.51 ± 0.01	2.52
	300°		2.45

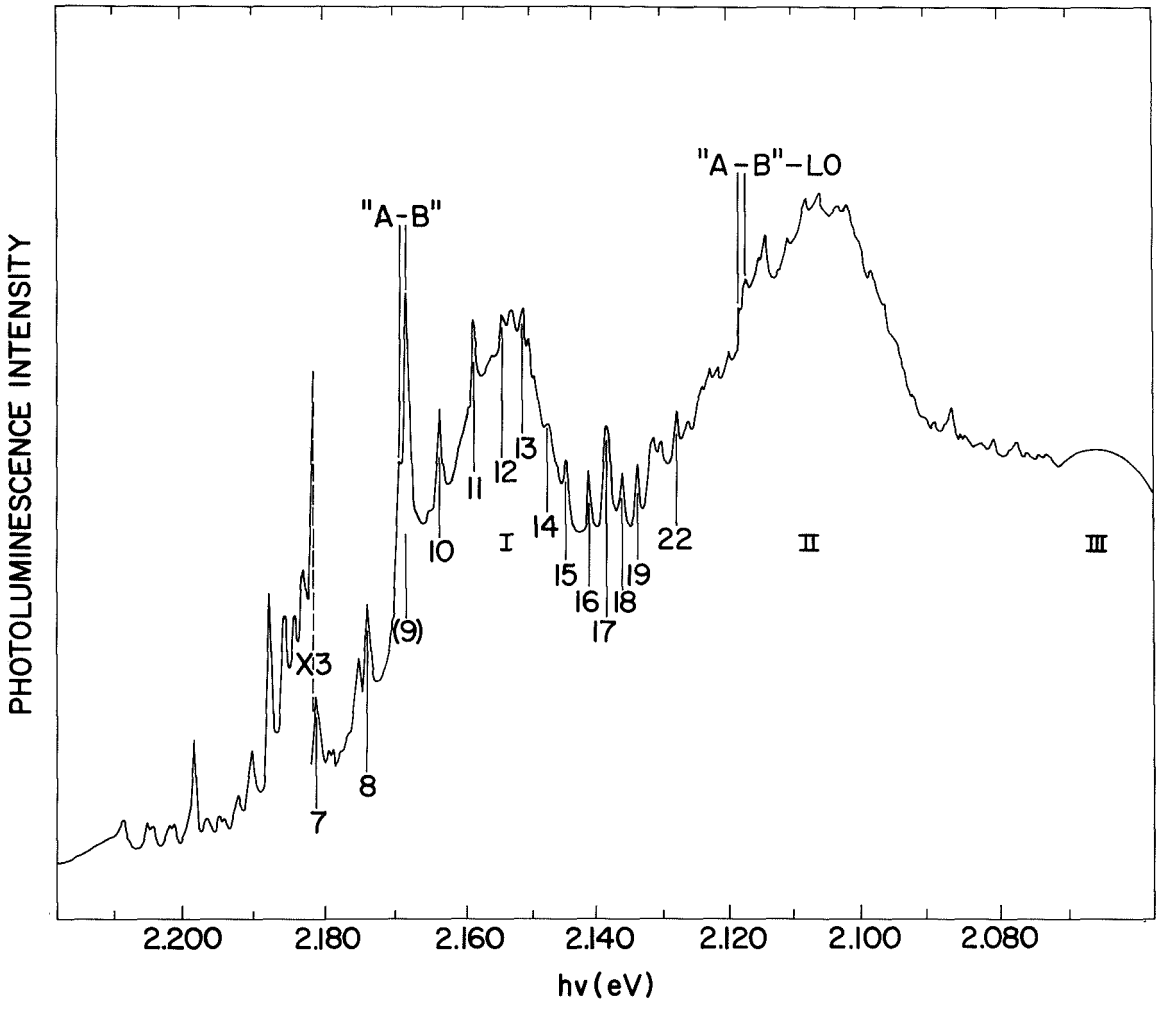

FIGURE IX

Donor-acceptor pair emission at 2°K of Zn doped AlAs.

$h\nu = E_g - (E_D + E_A) + \frac{e^2}{\varepsilon r}$. In Fig. 10 we have plotted the energy position of only those lines introduced by doping with Zn vs $\frac{1}{r}$ (r being the donor-acceptor pair separation) assuming the donors and acceptors are on opposite lattice sites, i.e., type II pair spectra. We have indicated shell assignments for the higher energy lines of the series and it can be seen that the agreement is good up to at least shell number 24. The gap in the series at shell number 9 can be explained as due to the presence of the two strong lines occurring at 2.16 eV and 2.1684 eV (Lines A-B, Fig. 2). This doublet, which is probably excitonic in origin, has a phonon replica at 2.118 eV and 2.1169 eV, which gives a value of 51.5 meV for the longitudinal phonon energy. These lines are not connected with the pair line systems since their relative intensities vary from sample to sample.

From the slope of the line joining the points in Fig. 10 we can calculate for AlAs an effective dielectric constant, ε, of 11.8. A more accurate value has been obtained recently from index of refraction measurements[5] which places the static dielectric constant at 10.06 ± 0.04.

The positions of the broad pair bands enable us to set limits on the values for the donor and acceptor binding energies associated with each peak. These are shown in the following Table.

Pair Band	Peak $h\nu$ (eV)	(E_g - $h\nu$ Peak)
I	2.150	.088
II	2.100	.138
III	2.060	.178

Since the addition of Zn introduces a type II pair spectra, the undoped AlAs must contain a donor impurity which occupies an As site. This strongly suggests a group VI element, most probably sulfur. If this same donor is associated with the pair band emission of Peaks I and II, we can set some limits on the individual binding energies: donor binding energy < .088 eV; acceptor (band II) binding energy > .050 eV; acceptor (Zn binding energy > .090 eV. These energies would be correspondingly increased by the $\frac{e^2}{\varepsilon r}$ addition if we knew the pair separation corresponding to the pair band maximum.

The Dependence of the Energy Gap and Conduction Band Structure Composition in the Ternary Alloys.- Alloy semiconductors are beset by three sets of problems. First is the problem of preparing the material. It is difficult and sometimes impossible to prepare large single crystal samples of uniform composition by any method. The second set of problems comes in defining the composition of such less than perfect samples. Finally, the third set of problems consists of measuring the physical properties of these samples and relating them to alloy composition. A very convenient and powerful technique for simultaneous composition

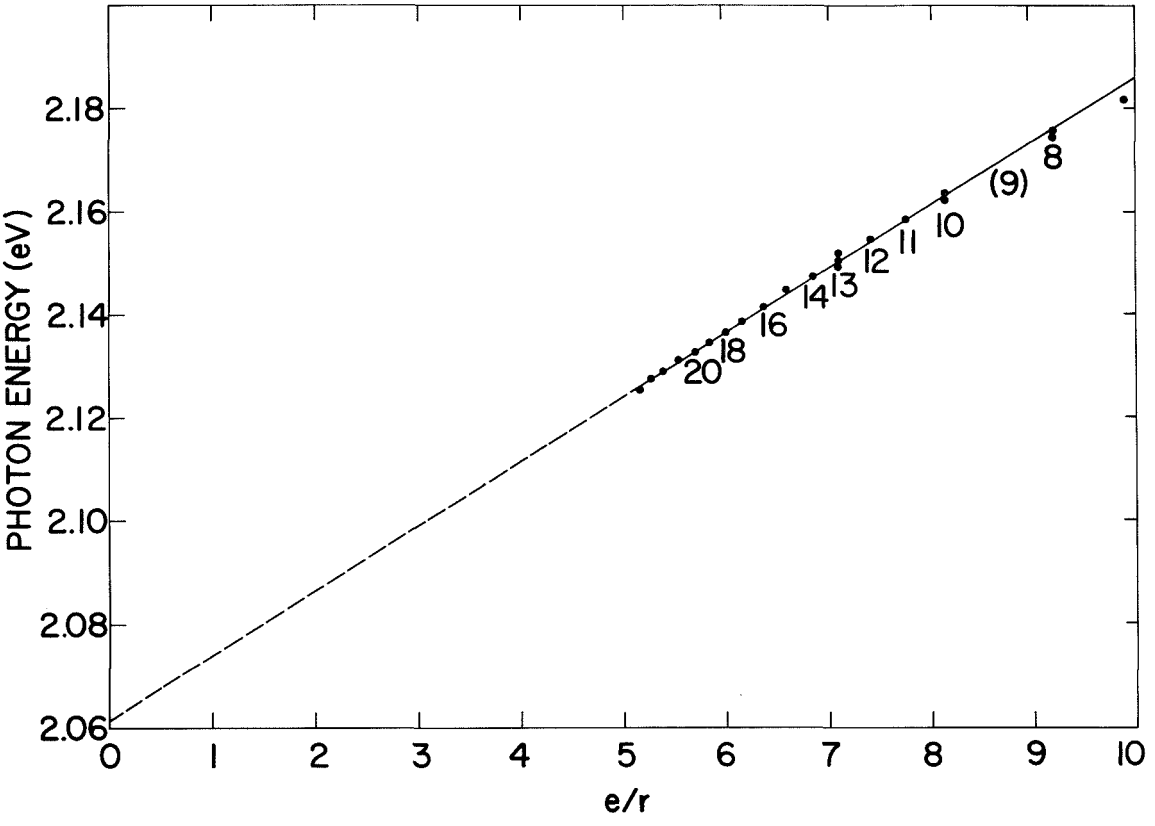

FIGURE X

Individual pair line energies attributable to unknown donor - Zn acceptor pairs as function of the reciprocal pair separation.

analysis and alloy band structure measurement is the quantitative analysis of x-ray emission and measurement of cathodoluminesence by a focussed electron microprobe beam. We have used this technique to study the $In_{1-x}Al_xP$ and $In_{1-x}Al_xAs$ ternary alloy systems.

The composition was determined by analysis of x-ray emission generated by an electron beam focussed down to about a 0.5 μm diameter using an EMX-SM Applied Research Laboratories electron microprobe. The cathodoluminescence, CL, was measured simultaneously on the electron microprobe using a monochromator and photomultiplier. The x-ray emission produced by the electron beam was analyzed to yield alloy compositions while simultaneously the visible and near-infrared luminescence was analyzed by a Perkin-Elmer model 98 monochromator with a DF glass prism, the detector being either an S-20 or S-1 photomultiplier. A 12-kV electron beam with a sample current of about 3×10^{-8} A was used. The electron beam was focussed to a spot of about 0.5 μ in diameter. The composition analysis was based on the intensities of the InL_α, AlK_α, AsL_α and PK_α lines in the alloy, elemental standards, and InP, AlAs, and AlP. The raw x-ray data were corrected for electron back-scatter and penetration and for x-ray absorption; the effect of secondary fluorescence was found to be negligible.

The CL spectra of $In_{1-x}Al_xP$ at room temperature for various values of the composition parameter x are shown in Fig. 11. The maximum intensity for each composition, x , is normalized to the same value. The spectral resolution in these measurements, constant except for the x = 0.97 trace, was such that no more than about 10 meV of the linewidths shown ($\sim$ 60 meV) is attributable to limited spectral resolution. Under definitely non-resolution-limited conditions linewidths of 45 to 50 meV have been observed in the room temperature CL of the same n-type InP used here. The fact that linewidths observed in the alloy are no wider than that of the InP is held as self-consistent evidence that the composition analysis and CL spectra are representative of homogeneous alloy material. In InP the CL peak is observable at 1.34 eV. This is close to the room temperature exciton gap of 1.3475 eV determined by Turner et al.[16] In the direct band gap range of the alloy system the Te-doped $In_{1-x}Al_xP$ CL peaks extrapolate perfectly to the CL peak of InP. Thus in the alloy the CL peak probably is within 10 meV of the energy gap as in InP. This CL peak has been plotted in Fig. 12 as a function of alloy composition and gives

$$E_{g\Gamma}(In_{1-x}Al_xP) = E_{g\Gamma}(InP) + 2.23x \text{ (eV)}.$$

With extrapolation beyond x = 0.5, this equation gives $E_{g\Gamma}$ for AlP as 3.6 eV.

The indirect (X-conduction band) gap is interpolated linearly between the gap in AlP (2.45) and the gap in InP (2.25 eV).[17] The direct and indirect conduction band minima are degenerate near x = 0.44 and E_g = 2.33 eV. The $In_{1-x}Al_xP$ alloy therefore has the highest direct gap of the III-V ternary alloy systems. These results on (In,Al)P have been published separately.[18]

In the design of alloy semiconductors to have as large a "crossover" energy as possible,[19] it has been pointed out that the zone center conduction band minimum of the direct gap semiconductor should be small and that the higher lying

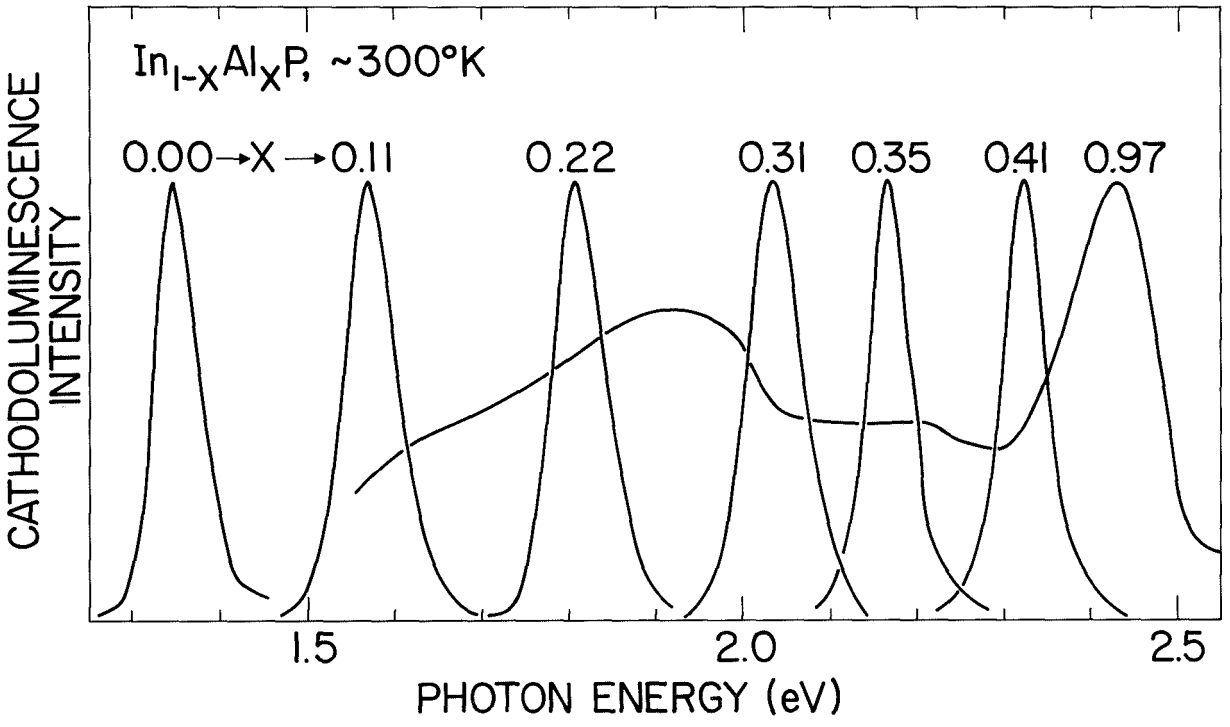

FIGURE XI

Cathodoluminescence spectra of $In_{1-x}Al_xP$ for various values of the composition parameter x. The spectra have been normalized to the same maximum value.

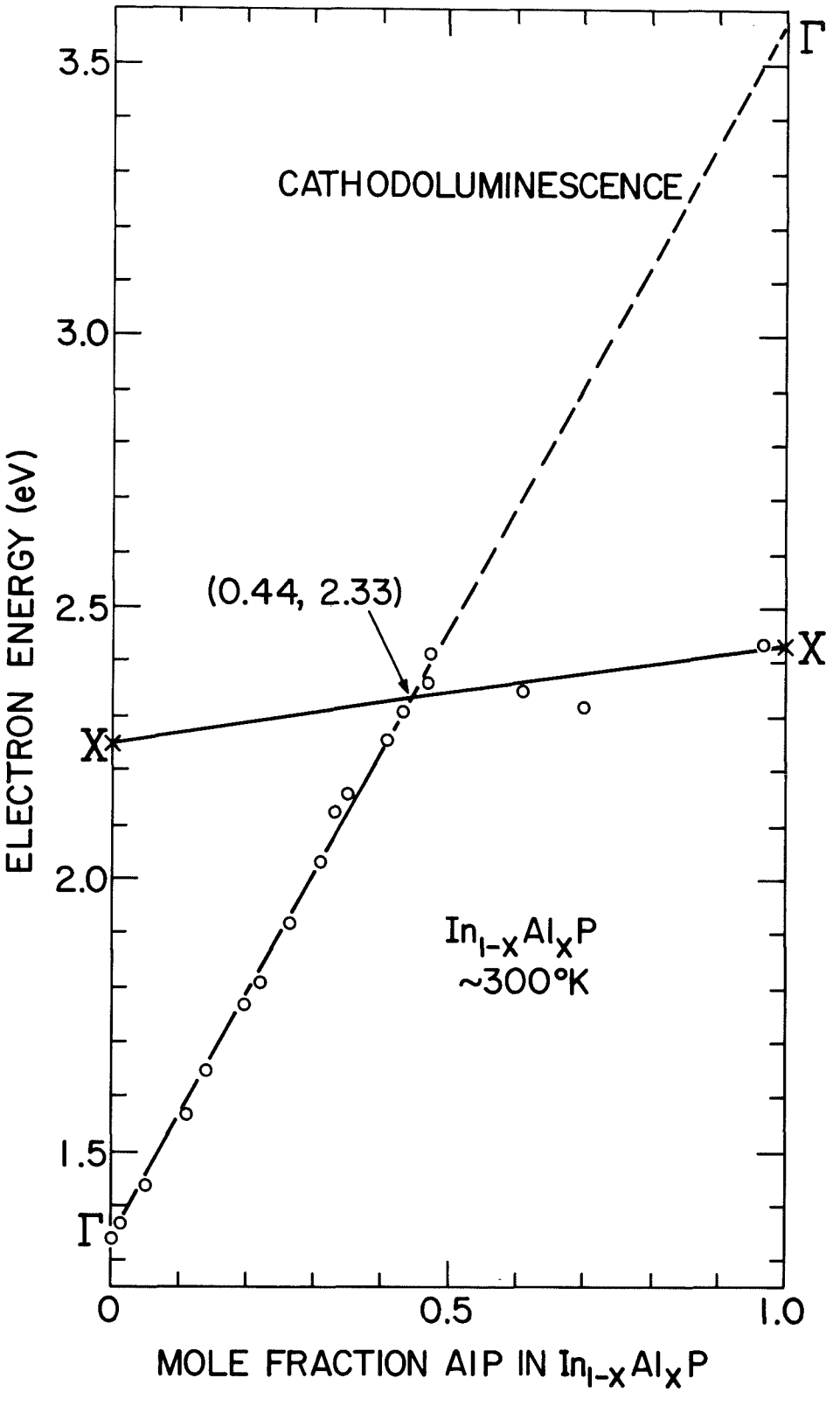

FIGURE XII

Cathodoluminescence peak energy versus alloy composition for $In_{1-x}Al_xP$. The lines have been drawn on the basis of about 30 data points; only the data obtained on one sample are shown in the interest of graphic clarity.

subsidiary minima should have as large an energy as possible. On this basis it was suggested that the $In_{1-x}Al_xAs$ system may have a crossover energy higher than that in the $Ga_{1-x}Al_x$ system even though the direct gap of InAs is much smaller than GaAs.[20] We have some limited data in the $In_{1-x}Al_xAs$ system which is shown in Fig. 13.

On the basis of the cathodoluminescence, the earlier prediction appears to be confirmed, i.e., $E_{\Gamma max}(Ga_{1-x}Al_xAs) = 1.92$ eV[21], 1.99 eV[22], versus $E_{\Gamma max}(In_{1-x}Al_xAs) = 2.05$ eV. The data in this system can also shed some light on the subsidiary minima in the InAs system. If we assume a linear indirect gap in the alloy, starting with $E_{gx} = 2.16$ eV in AlAs and passing through $E_{g\Gamma max} = 2.05$, an extension of the line to InAs predicts a value of 1.82 ± 0.1 eV for E_{gx} in InAs.

The conduction band minima of III-V compounds consistent with the alloy measurements and where possible measured independently are shown in Table IV.

DEVICE FABRICATION

1) Formation of p-n junctions by liquid phase epitaxy.- As described earlier, the growth of (Ga,Al)P is in general not as difficult as the growth of (In,Al)P. This is especially true for the LPE growth of thin layers of these ternary alloys on a substrate wafer, since GaP is a particularly suitable and readily available substrate for the growth of (Ga,Al)P. Thus, the primary objective of this phase of the research has been to obtain homogeneous epitaxial layers of (Ga,Al)P with high aluminum concentrations and to incorporate both donor and acceptor impurities for subsequent device evaluation.

Initially, a vertical liquid phase epitaxy process was used in an attempt to grow (Ga,Al)P epilayers. However, considerable difficulty was encountered in obtaining both p-type and n-type doping using this vertical LPE technique. In fact, we were only able to get n-type behavior by massive doping with silicon, and the p-type doping with zinc was uncertain due to the high background doping native to the growth process and apparatus. Considerable effort was expended in trying to develop and implement alternative methods to eliminate or considerably reduce effects caused by the volatility of these dopants (Te, Se, Zn, Cd, etc) at the rather high growth temperatures involved. Several new designs of the vertical liquid phase epitaxy process apparatus were tried, but no substantial improvement was noted. Other procedures were tried such as adding the elemental dopant just prior to epilayer growth and using solid phase aluminum compounds such as Al_2S_3 and Al_2Te_3 as doping sources. In each instance, the highly volatile nature of the dopant led to the rapid depletion of dopant in the melt resulting in a p-type epitaxial overgrowth.

In order to circumvent the inherent volatility of the commonly used dopants, we successfully applied a modified sealed system growth apparatus. The growth processes and growth variables were approximately the same for the sealed system technique as for the previous vertical liquid phase epitaxy technique, but with the difference that the dopant was confined to a relatively small isothermal volume and thus could not diffuse away and condense in a cooler region. Thus, difficulties associated with maintaining these highly volatile dopants in

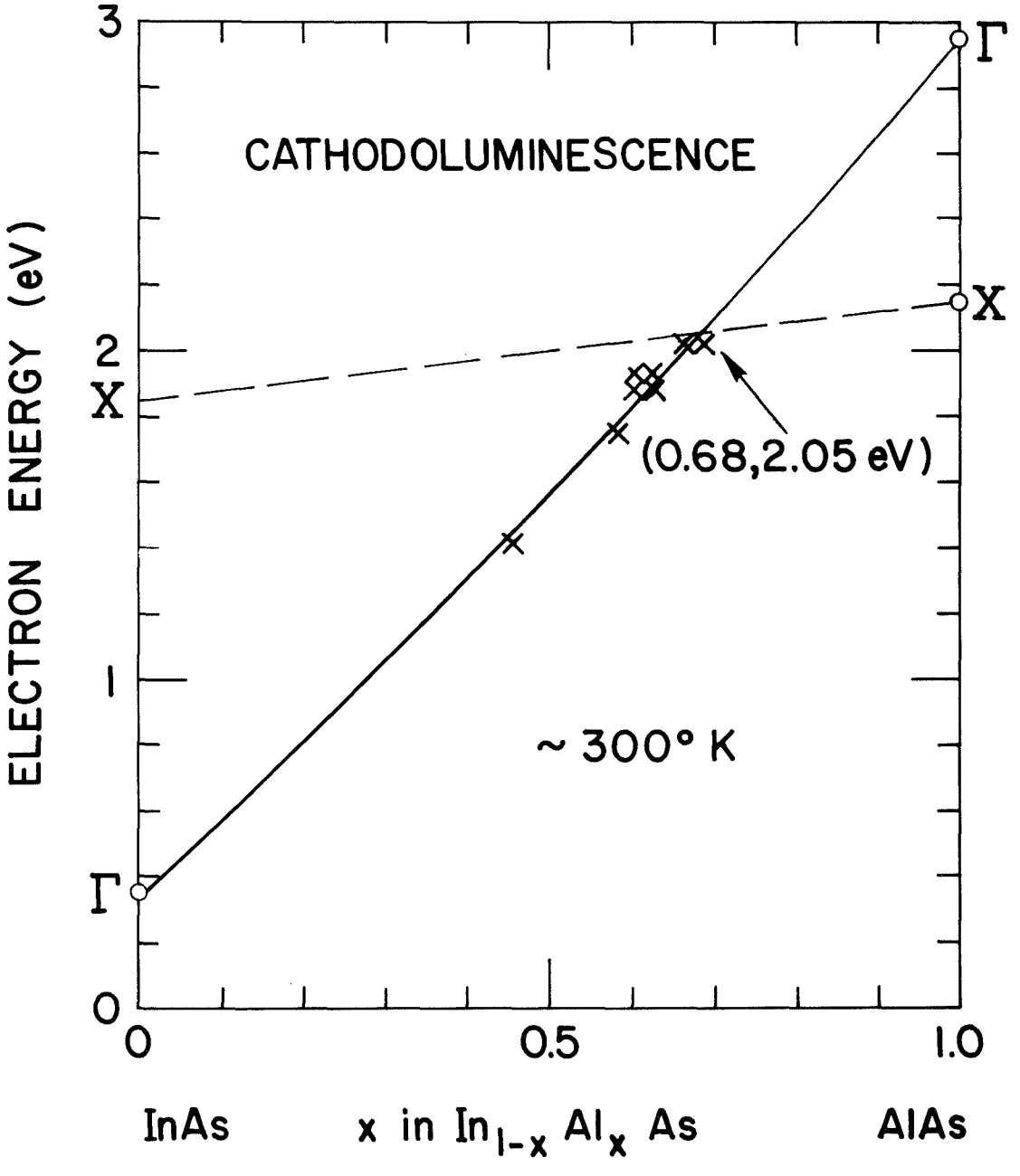

FIGURE XIII

Cathodoluminescence peak energies as a function of $In_{1-x}Al_xAs$ alloy composition at 300°K. The X conduction band has been extrapolated to InAs on the basis of the conduction band cross over point and the X point in AlAs.

TABLE IV

Conduction Band Energies (300°K)

Compound	$E_{g\Gamma}$	E_{gx}	E_{gL}
AlP	3.6[a]	2.45[g]	...
AlAs	2.95[b]	2.16[g]	...
GaP	2.78[c]	2.26[h]	...
GaAs	1.44[d]	1.87[i]	1.97[ℓ]
InP	1.35[e]	2.25[j]	...
InAs	0.36[f]	1.82[k]	...

REFERENCES

a) A. Onton and R. J. Chicotka, J. Appl. Phys. 41, 4205 (1970).

b) A. Onton, Proceedings of the Tenth International Conf. on the Physics of Semiconductors, Cambridge, Mass. 1970, p. 107.

c) P. J. Dean, G. K. Kaminsky, and R. B. Zetterstrom, J. Appl. Phys. 38, 3551 (1967).

d) M. D. Sturge, Phys. Rev. 127, 768 (1962).

e) W. J. Turner, W. E. Reese, and G. D. Pettit, Phys. Rev. 136, A1467 (1964).

f) S. Zwerdling, B. Lax, and L. M. Roth, Phys. Rev. 108, 1402 (1957).

g) M. R. Lorenz, R. J. Chicotka, G. D. Pettit and P. J. Dean, Solid State Communication 8, 693 (1970).

h) M. R. Lorenz, G. D. Pettit and R. C. Taylor, Phys. Rev. 171, 876 (1968).

i) I. Balslev, Phys. Rev. 173, 762 (1968).

j) W. P. Dumke, M. R. Lorenz, and G. D. Pettit, Phys. Rev. B1, 4668 (1970).

k) M. R. Lorenz and A. Onton, Proceedings of the Tenth International Conference on the Physics of Semiconductors, Cambridge, Massachusetts, 1970, p. 444.

ℓ) W. E. Spicer and R. C. Eden, Proceedings of the Ninth International Conf. on the Physics of Semiconductors, Moscow, 1968 (Nauke, Leningrad, 1968, p. 65). Their results indicate that E_{gL} is $\sim$ 0.1 eV higher than E_{gx}.

the solution are obviated. However, a minor disadvantage is also apparent: the vertical liquid phase epitaxy technique is an integrated technique wherein the melt may be easily counterdoped any number of times, while in the sealed system technique the melt cannot be counterdoped easily in one run. In order to first dope the epitaxial layer with a donor impurity and then subsequently with an acceptor impurity it is necessary to make two overgrowth runs.

The sealed system epitaxial solution growth process was used for preparing p-n junctions in (Ga,Al)P. The method consisted of enclosing within a sealed evacuated ampoule a long sealed crucible, one end of which contained a saturated Ga-GaP-Al melt together with the intentional dopant, the other end of which contained the substrate (GaP). Initially the substrate and the melt were not in contact, but were then caused to come into contact after equilibrium had been attained at an elevated temperature. This contact of the melt and substrate was caused by tipping the melt onto the substrate. Epilayer growth was then initiated by lowering the temperature of the saturated melt while the melt was in contact with the substrate. It was then necessary to repeat the above process using the alternate dopant.

All the components associated with the crucible and the crucible itself were made of pyrolytic BN. A schematic diagram of the crucible is shown in Fig. 14. The crucible was a hollow right circular cylinder sealed at one end. The crucible dimensions were 17 mm O.D. x 15 mm I.D. x 4 inches long. The open end of the crucible was sealed by using a tight fitting cap which prevented the melt from spilling when the crucible and charge were inverted. The GaP substrate was ultrasonically cut to fit the inside diameter of the crucible and was supported between a retaining ring and the crucible cap. A small hole 1/32" diameter was drilled midway along the length of the crucible so that the crucible could be evacuated within the quartz envelope. Typically the load up and growth of a crystal of composition $Ga_{0.3}Al_{0.7}P$ involved the following steps:

The BN crucible was held vertically and the charge of Ga 10 gms, GaP 700 mg, Al 55 mg and dopant was added (for an n-overgrowth $\sim$ 5 mg of Te was used). The GaP was added first in the form of small chunks; the Ga was then placed in the crucible followed by the addition of the Al and dopant. The BN retaining ring was then inserted and an n-type <111> oriented GaP substrate was placed on this support. The GaP substrate was inserted with the Ga face down. The BN cap was then put on, forcing the GaP substrate and retaining ring fully into the crucible. This ensemble was then placed within an 18 mm x 20 mm quartz tube together with a seal-off plug and was then evacuated. When the pressure in the system was approximately 10^{-6} Torr, the ampoule was heated by either a furnace or a hydrogen-oxygen torch to approximately 600°C. The system was then allowed to cool to room temperature and was sealed off. The ampoule was then positioned in a vertical furnace, was heated to 1070°C, and was then allowed to equilibrate at 1070°C for 1 1/2 hours. The furnace and ampoule were then rotated through 180°, causing the melt to contact the substrate, and then held at temperature for 15 minutes. The temperature was then raised 3°C and allowed to equilibrate for 30 minutes. The furnace was then cooled at a rate of 8°C per hour. When a temperature drop of 100°C had been realized, the cooling cycle was halted and the temperature was allowed to

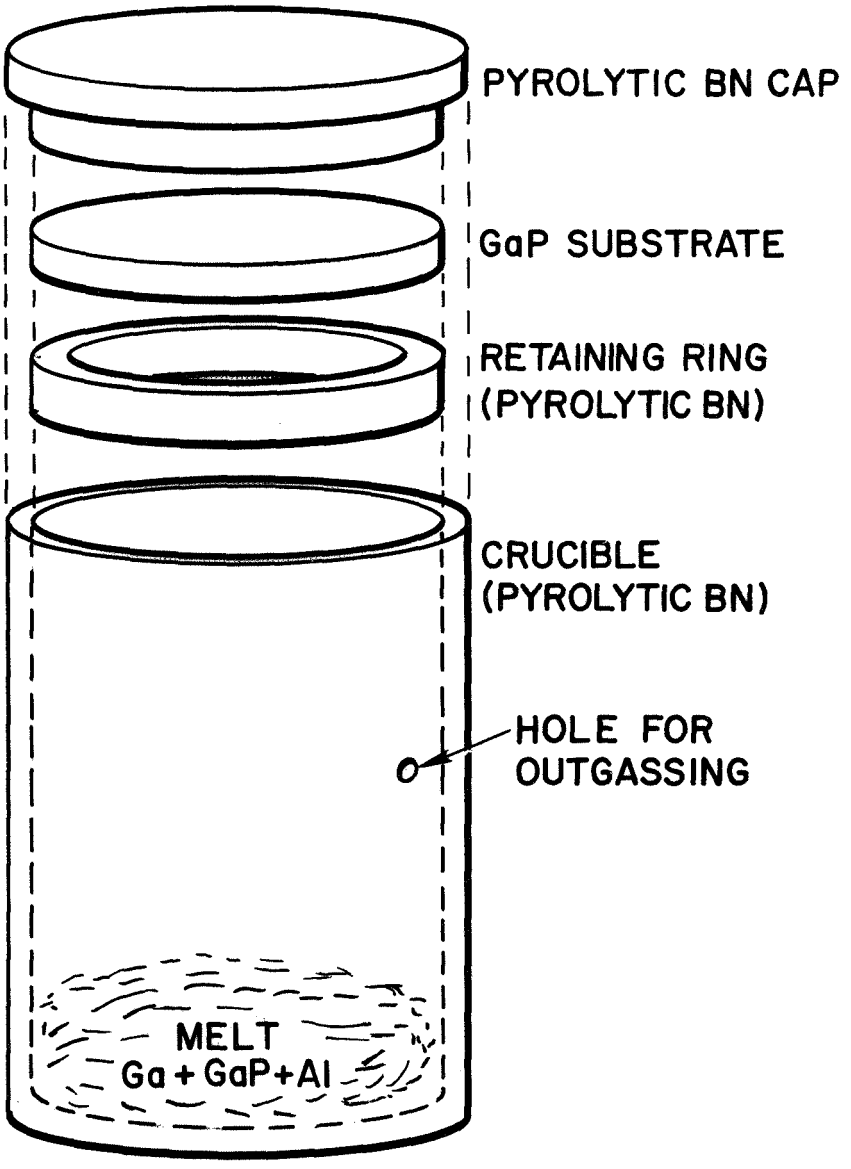

FIGURE XIV

Modified sealed system growth apparatus

remain constant at 973°C for 15 minutes. The furnace was again rotated through an arc of 180°C and then allowed to cool to room temperature. The substrate and doped epitaxial layer were then removed from the crucible. Any adherent Ga was removed from the epitaxial layer by scrubbing the surface with a cotton swab and warm acetone.

This substrate and n-doped epilayer then served as the substrate for the counter doped epilayer. Exactly the same procedure was followed except that the alternate dopant was added to the crucible (for a p overgrowth ∿ 25 mg Zn was added). The same cleaning step was then followed. The crystal was then cleaved (110 plane) at right angles to the overgrowth (111 plane). Microscopic investigation of such a cleavage plane at 90° to the surface reveals the hetero-junction plane and the p-n junction plane without any special treatment.

The composition of these (Ga,Al)P epitaxial layers was determined by electron microprobe analysis and the Al concentration was found to be essentially constant (decreasing only slowly with distance from the substrate). The Al concentration for all the doped $Ga_{1-x}Al_xP$ epilayers and p-n junction structures growth was greater than or equal to $x \cong 0.70$. Figure 15 shows a plot of the aluminum concentration x in the alloy $Ga_{1-x}Al_xP$ as a function of distance away from the GaP substrate into the epitaxial overgrowth. Electron microprobe data for two samples LPE-5 and LPE-8 are shown.

For sample #5 the initial mole fraction of aluminum in the melt was 0.028. The resulting solid has a composition of 0.91 Al and is essentially homogeneous in composition for 70 microns, dropping to a value of 0.88 mole fraction aluminim. Also this sample was stable in the atmosphere and showed no apparent signs of decomposition after 30 days in the laboratory environment. The initial mole fraction in the melt for sample #8 was 0.021. The resulting Al composition in the epitaxial layer was 0.77 mole fraction. The composition gradient found in the solid again is small and the epilayer is essentially constant in composition for the first 60 microns. At this point the composition changes from 0.73 to 0.17 mole fraction aluminum in the solid in approximately 2 microns. This is due to some of the melt being rapidly frozen at the termination of the epitaxial growth cycle. The segregation coefficient for aluminum is approximately 35 based on the initial composition of the epitaxial layer and on the aluminum composition of the melt.

Intentionally doped as well as nominally undoped layers of $Ga_{1-x}Al_xP$ with $x \geq 0.7$ mole fraction Al were grown using the sealed-system technique. Various donor, acceptor and amphoteric impurities were intentionally added to the crucible charge and the epilayers were grown onto semi-insulating substrates of GaP. Additional epilayers were also grown from charges to which no intentional dopant was added, so an estimate of the relative background impurity concentration could be made.

The donor dopants used were sulfur, tellurium and selenium; good single crystalline deposits were obtained with sulfur and tellurium doping. The selenium doped sample had many inclusions and could not be analyzed for physical and electrical properties. The acceptor impurities used were zinc and cadmium. Good characterization data could only be taken on the zinc doped epilayer.

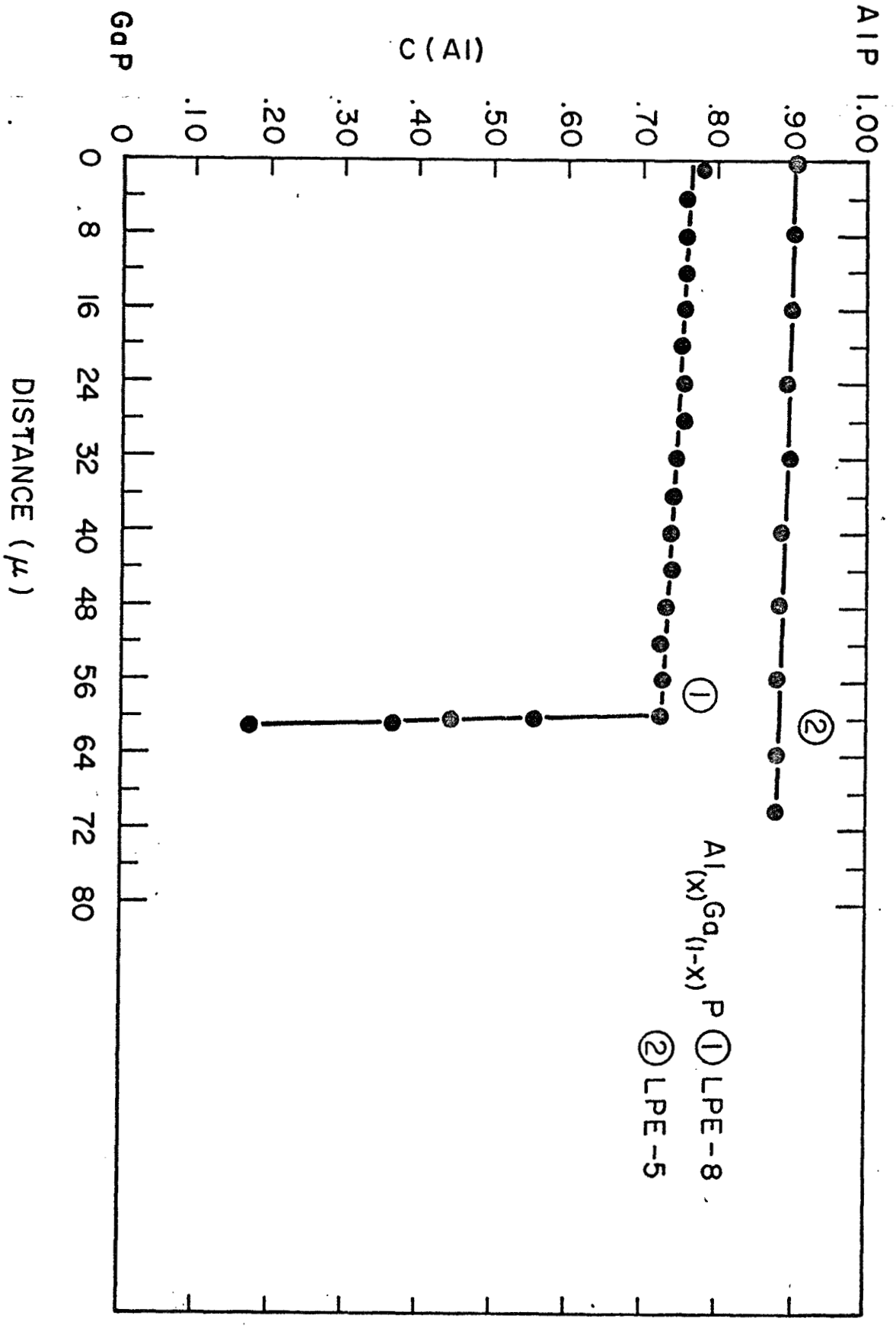

FIGURE XV

Composition of Al in $Ga_{1-x}Al_xP$ alloys as a function of distance away from the GaP substrate.

The cadmium doped samples were unsatisfactory. The amphoteric dopants used were silicon, carbon, tin and germanium. The carbon doped sample was grown in an all graphite system and a good epilayer was realized. The quality of the silicon doped and tin doped samples was also very good, the overgrowths being clear and transparent with no apparent inclusions. Germanium doped overgrowths could not be obtained with the horizontal LPE apparatus. However, some germanium doped samples were obtained with the earlier vertical LPE apparatus, but only on conducting substrates.

An estimate of the "effective electrical segregation coefficients" for some of the dopants was made and the results are shown in Table V. These "effective electrical segregation coefficients" were calculated by taking the ratio of the carrier concentration of the solid, as determined by electrical measurements, and the initial impurity concentration in the liquid. For these three dopants, the carrier concentrations in the samples grown were considerably in excess of the background levels obtained for nominally undoped materials.

2) Electrical Measurements.- Electrical measurements using the Hall technique were made on variously doped epitaxial layers of (Ga,Al)P. The problem of isolating the overgrowth layer from the substrate layer was overcome by growing the epilayers onto semi-insulating chromium doped GaP substrates. The substrates used were checked both before and after the overgrowths were made by reverse breakdown probe measurements and were verified to have remained semi-insulating. Single crystal Hall samples were ultrasonically cut from the overgrowth layers and electrical contact was made using either an eight point pressure contact Hall specimen holder or by alloying ohmic contacts to the samples.

Good ohmic contacts have been made to samples of $Ga_{1-x}Al_xP$ with values of x ranging from x = 0 to x = 0.88 mole fraction aluminum. It was found that an Au-Ge eutectic with a composition of 88% Au and 12% Ge was satisfactory for room temperature and liquid nitrogen measurements. The eutectic alloy melts at 356°C, which is considerably lower than most of the alloys used to date. On solidification this alloy expands, resulting in "sprouting" rather than contracting into a ball. Thus the Au-Ge eutectic wets the $Ga_{1-x}Al_xP$ well and provides good mechanical and electrical contact.

Measurements were made at room temperature and at 77°K and representative results, some of which show the extremes of the variations observed, are shown in Table VI.

These values for the mobilities, carrier concentrations and resistivities of the (Ga,Al)P samples doped with S, Te, or Zn agree reasonably well with comparably doped samples of GaP. Although these mobilities are perhaps somewhat lower than for GaP, they are not substantially reduced as might have been expected.

However, the Sn doped sample shows an anomalously high mobility at room temperature. The reasons for this apparent anomaly are not known at present. Typically, the maximum n-type mobilities observed for "pure" GaP are in the 150 to 200 cm^2/V sec range at room temperature and are of the order of 1000

TABLE V

"EFFECTIVE ELECTRICAL SEGREGATION COEFFICIENTS" FOR VARIOUS IMPURITIES

Dopant	Type	Effective Segregation Coefficients
S	n	4.0
Te	n	0.033
Zn	p	0.006

TABLE VI

ELECTRICAL PROPERTIES

	300°K			77°K		
	ρ	μ	N	ρ	μ	N
undoped	0.204	130	2.2×10^{17} n	4.69	178	7.5×10^{15} n
	2.611	58	4.1×10^{16} n	29.09	325	6.6×10^{14} n
S	0.00576	36	3×10^{19} n	0.00999	37	1.6×10^{19} n
Te	0.0388	59	2.7×10^{18} n	0.0112	25	2.2×10^{18} n
	0.75	13	6.0×10^{17} n	14.55	124	4.3×10^{15} n
Zn	0.132	61	7.7×10^{17} p	0.087	390	1.5×10^{15} p
	0.365	97	1.8×10^{17} p	12.10	410	1.2×10^{15} p
Sn	0.189	420	8.1×10^{16} n	41.5	477	3.1×10^{14} n
Si	2.24	164	1.7×10^{15} n	8269	852	8.8×10^{11} n
C	0.373	62	2.7×10^{17} n	14.47	15	2.9×10^{16} n

to 2000 cm^2/V sec at liquid nitrogen temperatures. Further work on the Sn doped samples would be of interest since the mobilities measured in this material are so unusual. The Si doped sample also seems somewhat anomalous. The mobilities are close to those expected for GaP at the same doping levels, but are much higher than observed in this study for nominally undoped (Ga,Al)P. However, for all the amphoteric dopants, the level of doping observed was so low that reliable conclusions are not possible.

In summary, by suitable precautions it has been found to be possible to dope (Ga,Al)P with the donors S and Te and with the acceptor Zn and to control the level of this doping at values which would be expected to give good electrical properties to p-n junction diodes.

3) Optical Measurements.- Optical absorption measurements were made on a relatively thick overgrowth layer (LPE-36) which was removed from the substrate and mechanically polished to a thickness of 0.002 in. In Fig. 16 we have plotted the absorption coefficient raised to the one-half power as a function of the photon energy at 77°K and 300°K. Also shown for comparison is the room temperature absorption curve for AlP determined and reported previously. Using the same criteria to define the band gap for AlP as for GaP (i.e., where $\alpha = 20\ cm^{-1}$), we tentatively assign the band gap of this alloy to be 2.41 eV compared to $E_g = 2.45$ eV for pure AlP. Based on previous careful analyses of the compositions and composition gradients of similar overgrowths, we expect that the average composition of this alloy should be $Ga_{0.26}Al_{0.74}P$. If we assume a linear variation of the energy gap from GaP to AlP then 2.41 eV for the above alloy corresponds to x = 0.75, in very good agreement with the above estimate.

Shown in Fig. 17 are the photoluminescent spectra at 2°K of two LPE samples doped with Sn. Both samples show pair band type spectra which peak at 2.245 eV and 2.202 eV and at 2.300 eV and 2.275 eV respectively. For the two tin doped samples, the more aluminum rich has the higher photoluminescent frequency as expected. The large shift of $\sim$ 0.070 V corresponds roughly to what would be expected for the known change in aluminum mole fraction from $\sim$ 20% to $\sim$ 70% between these two samples. The shapes and halfwidths of these bands are similar to the donor-acceptor pair band spectra commonly observed in GaP, but do not exhibit sharp structure due to individual donor-acceptor pairs or due to phonons at low temperatures. Lacking sharp lines and sufficient information about possible other impurities, it is difficult to speculate on the origin of these bands. The shift downward from the band edge amounts to about 0.120 eV and, if this arises predominantly from the binding energy of the electron to the tin donor, it is a somewhat favorable indication for the use of this donor in LED's to improve their efficiencies (although a still larger binding energy would be desirable).

The luminescence spectra observed for a germanium doped sample may well have originated from the GaP substrate similarly to the samples described next and hence this may be an indication either that germanium is not an efficient recombination center or that the doping level was not very high.

Other photoluminescence measurements were also made on epitaxial samples doped with various combinations of Zn and Te or S and on nominally undoped

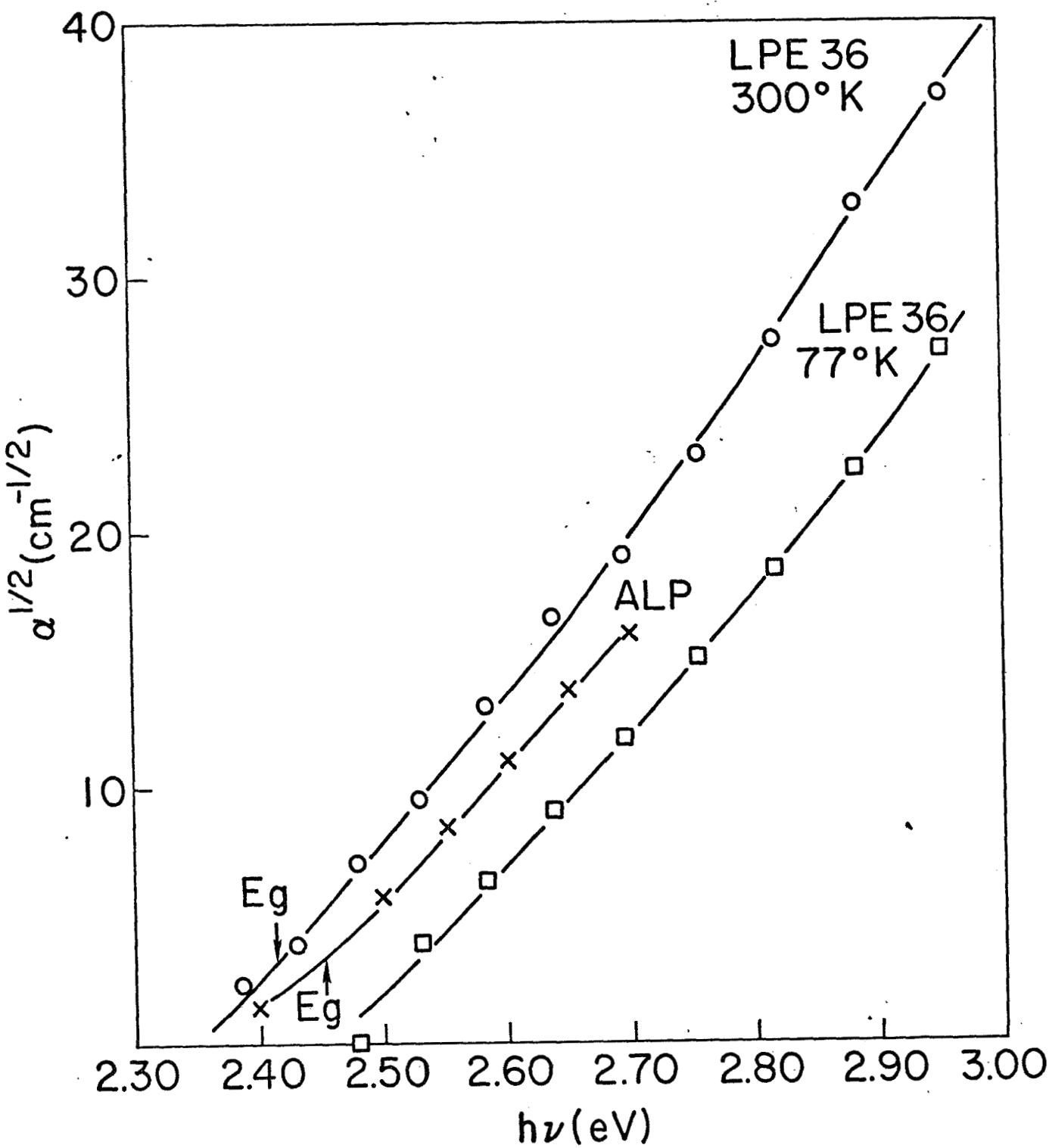

FIGURE XVI

The absorption curve at 300°K and 77°K for $Ga_{1-x}Al_xP$. Also shown for comparison is the room temperature absorption curve for AlP.

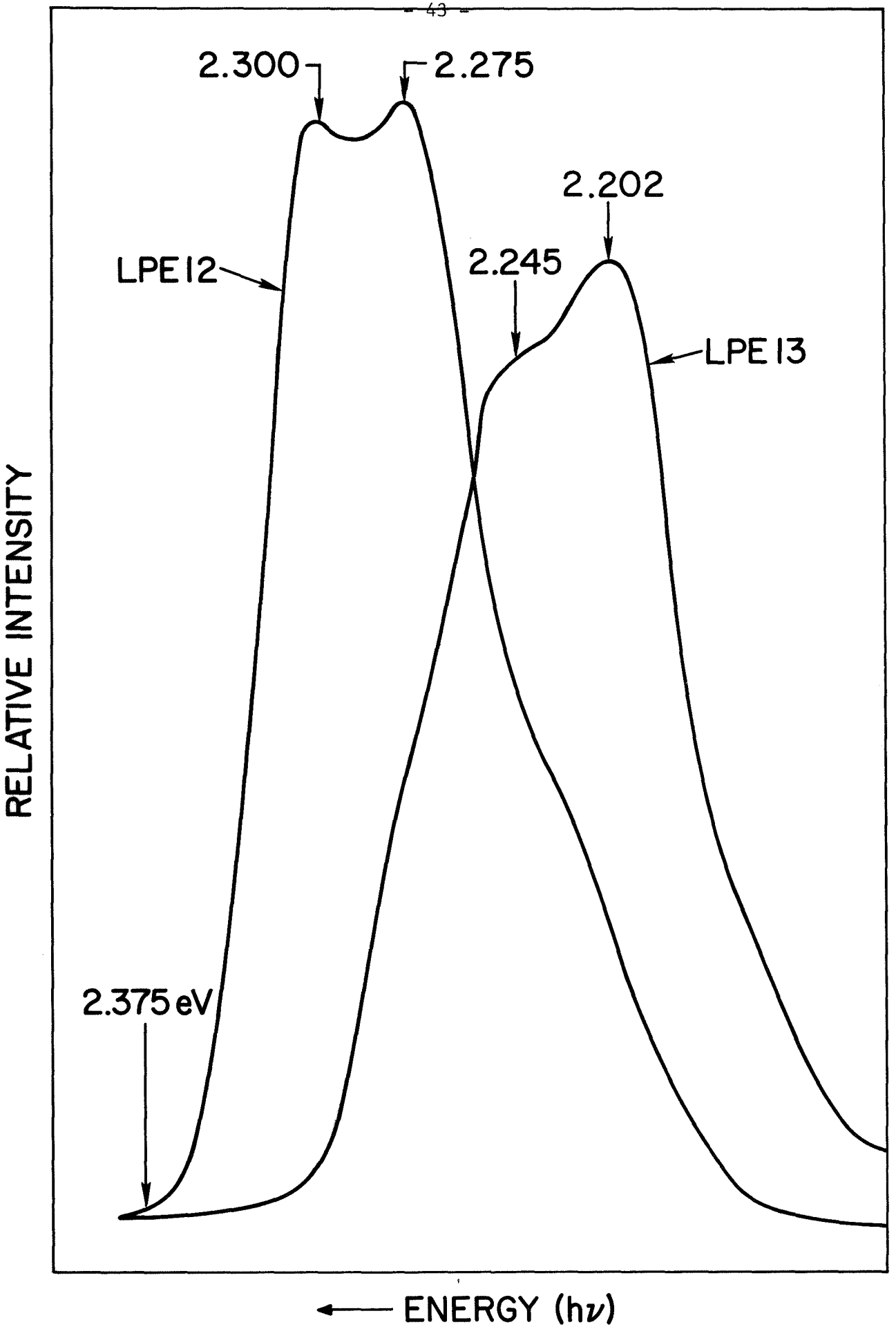

FIGURE XVII

The photoluminescence spectra at 2°K for two $Ga_{1-x}Al_xP$ samples doped with Sn.

samples. All these samples showed very similar spectra which resembled that for pure GaP with an emission peak at 2.192 eV. Two different excitation sources were used (the Ar 4880 Å line and the Hg 3650 Å line) in order to ascertain whether this effect could be due to the penetration of the excitation light to the GaP substrate. It appeared that this emission was somewhat weaker with the Hg excitation, which would be more heavily absorbed in the epilayer. However calibration of the intensity of the two sources was not performed and hence this observation is only a qualitative one. Thus, the observed luminescence probably originated from the GaP substrate and the luminescence from the doped eiplayer must have been so weak that it was not observed.

In summary, the LPE layers of (Ga,Al)P show the expected large band gaps in absorption measurements. Photoluminescence spectra were observed from the Sn doped samples, but not from the Zn, Te, S or Ge doped samples. As expected, this indicates that although use of Zn and Te or S to form a p-n junction will give good electrical properties they do not necessarily optimize radiative recombination processes. The decrease in the emission frequency of the Sn doped samples from the measured band edge appears to be on the order of 120 meV.

It would be expected that the emission from Sn as a donor on a group III site would be phonon assisted and hence would not be particularly strong. However, from our measurements to date, the strongest emission lines so far observed in photoluminescence are from tin doped material and hence tin might well enhance the efficiencies of LED's made from (Ga,Al)P.

4) Diffusion Studies.- Attempts have been made to incorporate Zn into n-doped $Ga_{1-x}Al_xP$ epilayers by diffusion. Epilayers doped with either Si or S were diffused under various conditions. Either elemental Zn or Zn_3P_2 were used as sources of the diffusant for diffusion into the Si doped layers (LPE-15). The Zn or Zn_3P_2 was loaded into an ampoule together with the $Ga_{1-x}Al_xP$ sample but physically separate from the samples. The ampoules were evacuated, outgased and sealed off. Diffusions were carried out at 700°C, 800°C, 900°C and 1000°C for various times. In each instance, the Zn diffused into the GaP substrate and the $Ga_{1-x}Al_xP$ epilayer. The surface of the epilayer degraded during the diffusion and this extended into the epilayer and terminated at the diffusion front. The GaP substrate did not degrade during diffusion at the lower temperatures, but was badly pitted at 1000°C. The diffusion depth for the Zn into $Ga_{1-x}Al_xP$ was approximately 1/3 of that of pure GaP. No light emitting diodes could be made from the diffused junctions, although diode characteristics were observed with high breakdown voltages.

Additional diffusions have been made into S doped (LPE-36) $Ga_{1-x}Al_xP$ epilayers using an Ga-Zn mixture as a diffusant source. Diffusion has been carried out at 800°C and 900°C for 16 hours. The diffusion depths were very shallow, however, indicating that either higher temperatures or longer diffusion times are necessary. There was apparently no surface degradation of the $Ga_{1-x}Al_xP$ layers. In view of the fact that good p-n junctions can be made by LPE methods, further diffusion studies were terminated.

5) Diode Contacting and Mounting.- Most of the substrate side of the crystal was lapped off, leaving a thickness of about 8 mils so that the crystal could be easily cleaved into small triangular platelets less than 1 mm on an edge. Ohmic contacts to the crystal were made by simultaneously alloying a tab of In 5% Au alloy into the p-side and a tab of Au 38% Sn into the n-side in a stream of forming gas. The alloying was done on a hot stage at an alloying temperature of about 360°C. The sample was held at this temperature for not more than a few seconds. The crystal with contacts was then mounted on a conventional header (TO-5).

Some of the various combinations of dopants used for these diodes and their concentrations are shown in Table VII. These overgrowth runs were all successful and representative diodes could be fabricated from the epitaxial layers. These epilayers were all grown by the sealed-system technique except for LPE-25, which was grown by the vertical liquid phase epitaxy process. The doping levels in the crystal shown for the Zn and Te dopants were determined a posteriori based on the segregation coefficients for these dopants previously given in this report. For the samples doped with nitrogen via NH_3, it was estimated that the melt composition was approximately 2×10^{19} atoms/cm^3. Some samples were doped simultaneously with B and Sb on the n-side and the melt concentrations are given in Table VII. No estimate of the amount of B and Sb incorporated in the crystal lattice has been made.

A number of diodes have been made of $Ga_{1-x}Al_xP$ material with $x \geq 0.7$ and with different levels of Te and Zn doping. It was found that such diodes when grown on p-type GaP substrates had optimum electrical and radiative properties when the Te carrier concentration was $\sim 1 \times 10^{18}$/cm^3 and the Zn carrier concentration also was $\sim 1 \times 10^{18}$/cm^3. Such diodes emitted easily visible greenish-blue light.

The emission spectra of several such diodes were measured and the spectrum at 300°K for one of the diodes is shown in Fig. 18; the emission spectra at 77°K is shown in Fig. 19. The room temperature measurements were made with the diodes biased in the forward direction at 100 m.a. The high energy emission band with the peak at 2.385 eV had a width at half intensity of about 150 meV. The peak energy of the diodes was independent of applied voltage and occurred at approximately 30 meV below our estimate of the band gap. This band gap energy was separately determined on a similarly grown sample of approximately the same composition (see Fig. 16). A very broad emission was also present centered at 1.58 eV.

The high energy emission (2.385 eV) is tentatively interpreted as being an exciton type recombination because of its similarity to that seen in GaP. For example, in GaP the exciton bound to N substituted on P sites occurs at 30 meV below the band gap in electroluminescence, has a width at half intensity of 75 meV and is voltage independent.

The ratio of the peak heights of the high energy peak to the infrared peak varied from 0.1 at 5 ma to 0.6 at 100 ma. This is in agreement with the expected behavior. The brightness of the diodes was 20 foot-lamberts at

TABLE VII

Diode	Dopant and Doping Level	Substrate
LPE - 25	Te: 5×10^{17}; Zn: 8×10^{17}	n GaP
- 35	Zn: 4×10^{18}; Te: 2×10^{18}	p GaP
- 38	Zn: 1×10^{18}; Te: 1×10^{18}	p GaP
- 48	Te: 1×10^{18}; Zn: 1×10^{18} (NH_3)	n GaP
- 54	Zn: 1×10^{18}; Te: 2×10^{17} (NH_3)	p GaP
- 58	Zn: 1×10^{18}; Te: 5×10^{16} (NH_3)	p GaP
- 58	Heat treat at 700°C for 1 hour	
- 62	Zn: 8×10^{17}; Te: 2×10^{17} (BSb: 3×10^{20})	p GaP
- 62	Heat treat at 800°C for 4 hours	
- 66	Zn: 7×10^{17}; Te: 2×10^{17} (BSb: 5×10^{19})	p GaP
- 67	Zn: 6×10^{17}; Te: 3×10^{17} (BSb: 5×10^{18})	p GaP

All of the above epitaxial overgrowths were grown having an average composition $Ga_{0.3}Al_{0.7}P$ except for LPE-48 which contains no Al.

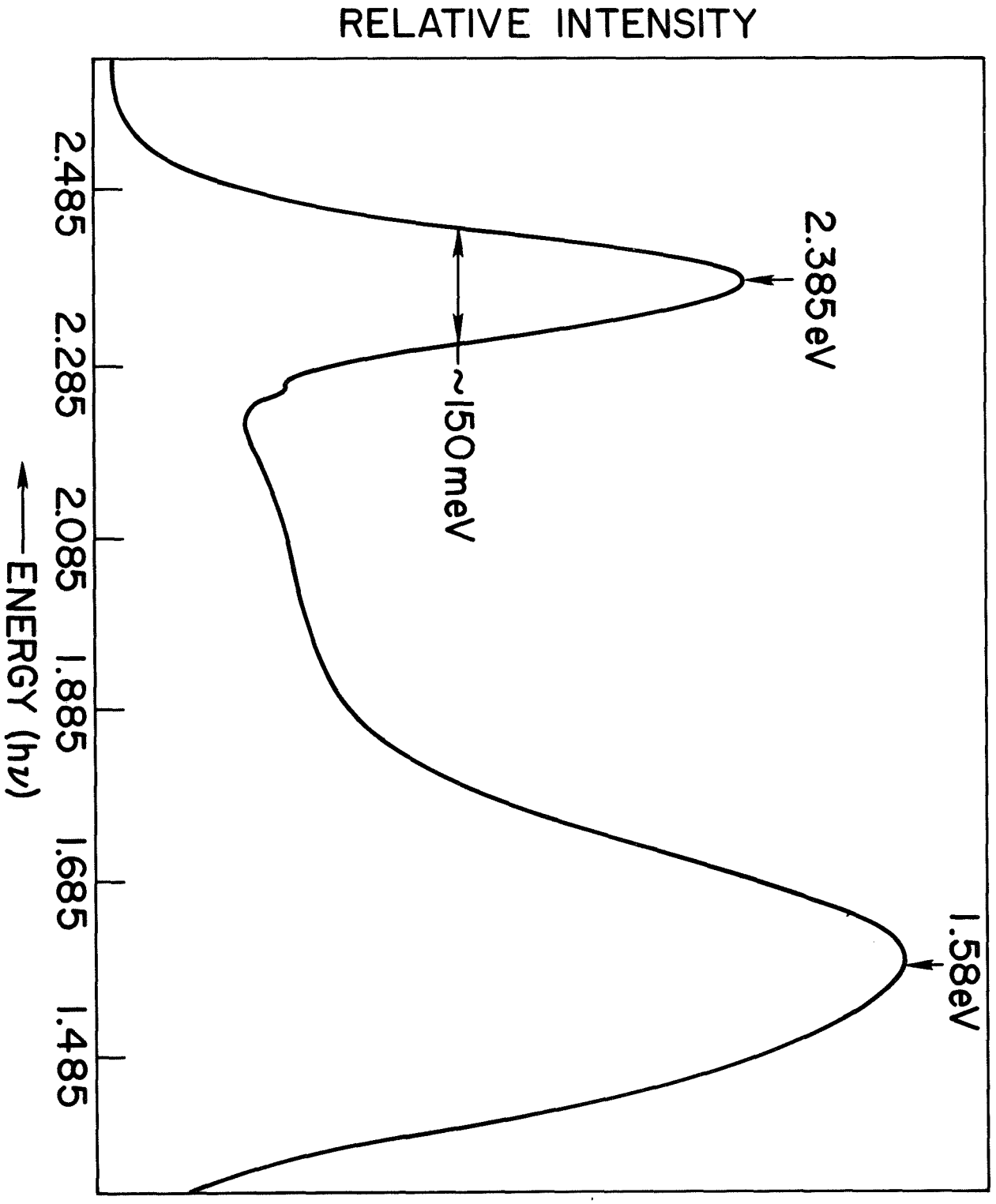

FIGURE XVIII

The emission spectrum at 300°K for a $Ga_{1-x}Al_xP$ Te-Zn doped diode.

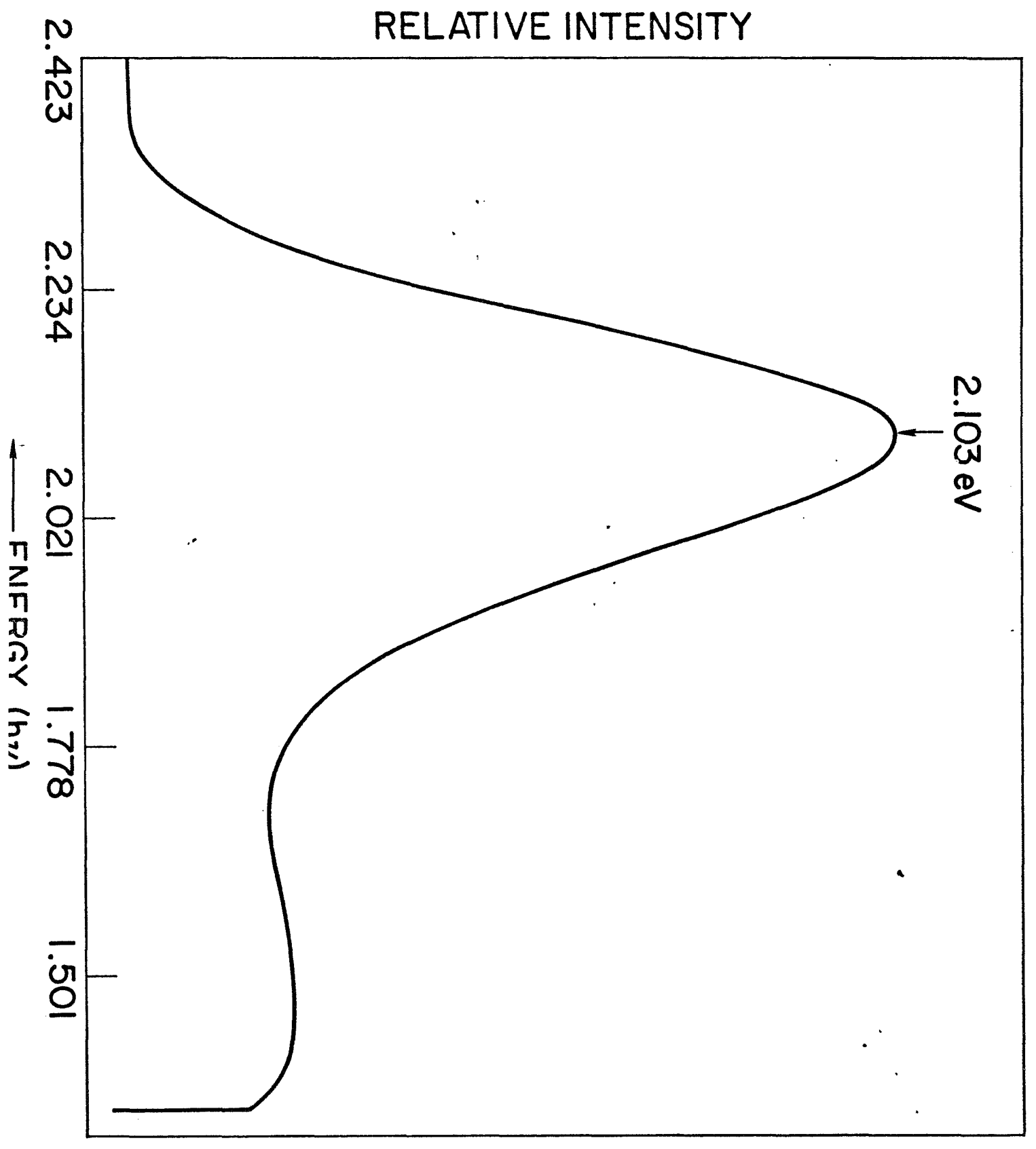

FIGURE XIX

The emission spectrum at 77°K for the same $Ga_{1-x}Al_xP$ diode.

50 ma with external quantum efficiencies of approximately 2×10^{-5}. Such efficiencies are fairly comparable to those originally observed for green donor-acceptor doped GaP. Efficiencies of up to 0.1% have been observed for improved S and Zn doped GaP low resistance diodes with a very good brightness. There is no apparent reason why with further development similar improvements could not be made for these (Ga,Al)P diodes.

At 77°K (see Fig. 19) there was only a single dominant peak and this occurred at 2.100 eV. The halfwidth was 115 meV and the peak was voltage independent. No interpretation has been made as yet as to the origin of this emission.

Measurements on the N doped and on the B and Sb doped crystals are as yet so fragmentary that no conclusions can be drawn about the effects these dopants have on the radiation emitted by these diodes.

The results on the Te and Zn doped diodes are encouraging since it has been demonstrated that it is possible to fabricate p-n junction diodes from (Ga,Al)P material which have good electrical properties and which emit light of a substantially higher frequency than can be obtained from GaP. Although the efficiencies so far obtained are relatively low, improvements in the LPE growth technique or in the amount and type of dopants might well be expected to lead to a greatly improved efficiency of light emission. Hence a brightness of 20 foot-lamberts can be considered a favorable indication that (Ga,Al)P has the potential for overcoming some of the limitations of presently used III-V materials if more favorable dopants can be identified to optimize the light emission properties of this material.

CONCLUSIONS AND RECOMMENDATIONS

It has been found possible to grow bulk crystals of the compounds AlAs and AlP and, by studying their optical properties, to measure and to understand their band structures and some of the radiative transition processes which can occur in these compounds.

Similarly, it has been possible to grow crystals of the ternary alloys (In,Al)As and (In,Al)P and to study their band structures as a function of alloy composition. For the former, the radiative transitions remain direct up to the "crossover" point at the composition $In_{.32}Al_{.68}As$ where the band gap is 2.05 eV. For the latter, the "crossover" point occurs at $In_{.56}Al_{.44}P$ and a band gap of 2.33 eV. This is the highest direct band gap energy known in a III-V compound or alloy which can be readily doped both p-type and n-type.

However, from information obtained on the phase diagrams of these (In,Al)V alloys and from our experience in growing these two alloys, it is apparent that it is not possible to reproducibly grow by any melt or solution technique reasonably homogeneous bulk crystals or epitaxial layers which have a <u>direct</u> band gap and which would be useful in device application.

Both bulk crystals and epitaxial layers of (Ga,Al)P were grown and it was possible to reproducibly grow homogeneous epitaxial layers of this alloy in the highly AlP rich range. Such layers were doped p-type with zinc and

n-type with sulfur or tellurium and p-n junction diodes were formed which emitted greenish-blue light with a peak energy at 2.385 eV.

It is recommended that subsequent work should concentrate on the (Ga,Al)P alloy rather than the (In,Al)P alloy. Although it should be possible to grow sufficiently homogeneous and reproducible epitaxial layers of either material in the highly aluminum rich indirect band gap range, the difficulties of providing a compatible substrate for (In,Al)P and the possible adverse effects of localized lattice strains arising from the disparity in the size of the In and Al atoms make (In,Al)P the less promising material.

It should be possible to substantially improve the efficiencies of the (Ga,Al)P diodes doped with Zn and Si or Te from the present values of $\sim 2 \times 10^{-5}$ by optimizing both dopant concentrations and the epitaxial growth conditions (similar GaP diodes exhibit efficiencies of $\sim 10^{-3}$ at 2.190 eV). Such work is at present only in its very early stages and a careful investigation should be made to establish the radiative mechanisms and the binding energies connected with these dopants.

The major direction of subsequent work on (Ga,Al)P should be to identify dopants which have substantially deeper binding energies than S or Te and which form efficient radiative recombination centers. Although there is no assurance that such dopants exist for (Ga,Al)P, there are several possibilities which should be carefully explored. If this search is successful, light emitting diodes made from this alloy material should be considerably brighter than any diodes presently available.

Papers Published or Submitted Under Contract NAS 12-2169

1. "The Fundamental Absorption Edge of AlAs and AlP," M. R. Lorenz, R. J. Chicotka, G. D. Pettit, and P. J. Dean, Solid State Comm. 8, 693 (1970).

2. "Conduction Bands in $In_{1-x}Al_xP$," A. Onton and R. J. Chicotka, J. Appl. Phys. 41, 4205 (1970).

3. "Electronic Structure of III-V Alloys from Luminescence," M. R. Lorenz and A. Onton, Proc. Tenth International Conf. Physics Semiconductors, Cambridge, Mass., 1970, p. 444.

4. "Solidus Boundary in the GaAs-AlAs Pseudobinary System," L. M. Foster, (to be submitted for publication).

5. "Solidus Boundary in the InAs-AlAs Pseudobinary System," L. M. Foster and J. E. Scardefield, J. Electrochem. Soc. 118, 495 (1971).

6. "The Effect of Higher Lying Conduction Band Minima on the Optical Absorption in GaP and AlAs," W. P. Dumke, M. R. Lorenz, and G. D. Pettit, (Submitted for publication).

REFERENCES

1. L. M. Foster and J. E. Scardefield, J. Electrochem. Soc. 117, 534 (1970).

2. L. M. Foster and J. F. Woods, J. Electrochem. Soc., to be published (July 1971).

3. L. M. Foster (to be submitted for publication).

4. L. M. Foster and J. E. Scardefield, J. Electrochem. Soc. 118, 495 (1971).

5. R. E. Fern and A. Onton, J. Appl. Phys., to be published.

6. C. A. Mead and W. G. Spitzer, Phys. Rev. Letters 11, 358 (1963).

7. R. J. Elliott, Phys. Rev. 108, 1384 (1957).

8. P. J. Dean, J. Luminescence 1,2, 398 (1970).

9. J. C. McGroddy, M. R. Lorenz, and J. E. Smith, Jr., J. Appl. Phys. 42, 1852 (1971).

10. P. J. Dean and D. G. Thomas, Phys. Rev. 150, 690 (1966).

11. G. G. MacFarlane, T. P. McLean, J. E. Quarrington, and J. Roberts, J. Phys. Chem. Solids 8, 388 (1959).

12. W. Kischio, Z. Anorg, Allgem. Chem. 328, 187 (1964).

13. M. R. Lorenz, R. J. Chicotka, G. D. Pettit, and P. J. Dean, Solid State Comm. 8, 693 (1970.

14. S. Z. Beer, J. F. Jackovitz, D. W. Feldman, and J. H. Parker, Jr., Phys. Letters 26A, 331 (1968).

15. W. P. Dumke, M. R. Lorenz, and G. D. Pettit (submitted for publication).

16. W. J. Turner, W. E. Reese, and G. D. Pettit, Phys. Rev. 136, A, 1467 (1964).

17. W. P. Dumke, M. R. Lorenz, and G. D. Pettit, Phys. Rev. B1, 4668 (1970).

18. A. Onton and R. J. Chicotka, J. Appl. Phy. 41, 4205 (1970).

19. M. R. Lorenz, Proceedings of the Conference "Materials and Characterization," Chania, Crete, 1969.

20. M. R. Lorenz and A. Onton, Proc. Tenth International Conf. Physics Semiconductors, Cambridge, Mass. 1970, p. 444.

21. H. C. Casey, Jr. and M. B. Panish, J. Appl. Phys. 40, 4910 (1969).

22. A. Onton, M. R. Lorenz, and J. M. Woodall, Bull. A. Phys. Soc. II, Vol. 16, 371 (1971).